



## OPEN ACCESS

## EDITED BY

Christian Marcelo Ibáñez,  
Andres Bello University, Chile

## REVIEWED BY

Catarina Araújo-Silva,  
Federal University of Pernambuco,  
Brazil  
Juliana Lopes Segadilha,  
Federal University of Rio de Janeiro,  
Brazil

## \*CORRESPONDENCE

Ferran Palero  
Ferran.Palero@uv.es

<sup>†</sup>These authors have contributed  
equally to this work

## SPECIALTY SECTION

This article was submitted to  
Marine Evolutionary Biology,  
Biogeography and Species Diversity,  
a section of the journal  
Frontiers in Marine Science

RECEIVED 23 April 2022

ACCEPTED 18 July 2022

PUBLISHED 02 September 2022

## CITATION

Gellert M, Palero F and Błażewicz M  
(2022) Deeper diversity exploration:  
New Typhlotanaidae (Crustacea:  
Tanaidacea) from the Kuril-Kamchatka  
Trench area.  
*Front. Mar. Sci.* 9:927181.  
doi: 10.3389/fmars.2022.927181

## COPYRIGHT

© 2022 Gellert, Palero and Błażewicz.  
This is an open-access article  
distributed under the terms of the  
[Creative Commons Attribution License  
\(CC BY\)](https://creativecommons.org/licenses/by/4.0/). The use, distribution or  
reproduction in other forums is  
permitted, provided the original  
author(s) and the copyright owner(s)  
are credited and that the original  
publication in this journal is cited, in  
accordance with accepted academic  
practice. No use, distribution or  
reproduction is permitted which does  
not comply with these terms.

# Deeper diversity exploration: New Typhlotanaidae (Crustacea: Tanaidacea) from the Kuril- Kamchatka Trench area

Marta Gellert <sup>1†</sup>, Ferran Palero <sup>2,3\*†</sup> and Magdalena Błażewicz <sup>1</sup>

<sup>1</sup>Department of Invertebrate Zoology and Hydrobiology, Faculty of Biology and Environmental Protection, University of Lodz, Łódź, Poland, <sup>2</sup>Cavanilles Institute of Biodiversity and Evolutionary Biology, University of Valencia, Paterna, Spain, <sup>3</sup>Department of Life Sciences, The Natural History Museum, London, United Kingdom

Typhlotanaidae Sieg, 1984, is one of the most diverse Tanaidacea families from deep-sea waters. Its diversity is underestimated, and evolutionary relationships within the family remain mostly unknown. Deep-sea typhlotanoids collected from 23 sites across the Kuril-Kamchatka Trench and nearby waters were studied using an integrative taxonomy approach, combining morphological and genetic data (i.e., the mitochondrial subunit I of the cytochrome oxidase (COI) and the 18S rDNA nuclear gene). One new species of *Typhlamia* and two new species belonging to two new genera are described, significantly increasing the known diversity of typhlotanoids from the NW Pacific. The molecular phylogeny obtained, despite being preliminary results, was congruent with morphological data and supports the monophyly of different groups such as the 'short-bodied' forms (represented by *Ty. cornutus* and *Ty. eximius*) or the 'collar' forms (e.g., *Ty. variabilis* and *Torquella*). Molecular data confirm the non-monophyly of *Typhlotanais* species. Finally, the new typhlotanoid taxa seem to have distinct bathymetric distribution and ecological requirements, but further data on environmental factors and species abundances are still needed.

## KEYWORDS

Peracarida, deep sea, integrative taxonomy, Tanaidomorpha, DNA barcoding

## Introduction

Northwestern Pacific abyssal domains are productive, nutrient-rich marine bottoms with a unique fauna (Brandt et al., 2015; Saeedi and Brandt, 2020; Stępień et al., 2022). Complex topography and a convoluted oceanic current system, together with the intricate history of surrounding seas, have shaped their marine biodiversity, expressed in the astonishing richness and zoogeography pattern of multiple benthic groups

(Grebmeier et al., 2006; Renema et al., 2008; Leprieur et al., 2016; Kaiser et al., 2018; Bober et al., 2019; Saeedi et al., 2019; Jażdżewska et al., 2021a, 2021b). The series of R/V *Vitjaz* historic expeditions triggered the study of NW Pacific deep-sea macrofaunal communities (Sirenko, 2013; Brandt et al., 2015), but results of the recent investigations suggest that Peracarida taxa previously considered rare and unique may be in fact frequent and abundant on bathyal and abyssal ecosystems (Larsen and Shimomura, 2007; Brandt et al., 2010; Golovan et al., 2013; Malyutina et al., 2015; Jażdżewska and Mamos, 2019; Saeedi et al., 2019; Jażdżewska et al., 2021a).

Although Tanaidacea are an essential element of these deep-sea peracarid assemblages (Golovan et al., 2013; Brandt et al., 2015; McCallum et al., 2015; Poore et al., 2015), not much is known about their spatial distribution and bathymetric preferences (Brandt et al., 2013; Di Franco et al., 2021). Limited swimming abilities and lack of planktonic larval stages (Highsmith, 1985; Hassack and Holdich, 1987; Larsen, 2005) make them ideal model organisms for understanding dispersal and population connectivity (Błażewicz-Paszkowycz et al., 2014; Hilário et al., 2015). Indeed, recent studies have shown that topographic structures (e.g., sea mountains, fractures, or trenches) correlate with population connectivity on some tanaid genera (Jakiel et al., 2018; Jakiel et al., 2019; Jakiel et al., 2020), but this issue is still far from fully resolved.

Typhlotanaidae Sieg, 1984, is one of the most frequent and diverse Tanaidacea families in deep-sea waters, currently including 117 species classified into 13 genera (Błażewicz-Paszkowycz et al., 2012; Segadilha & Serejo, 2022). Most typhlotanuids are characterized by the presence of their clinging apparatus on pereopods 4–6, which facilitates individuals to move inside their tubular houses. The lack of this specialized set of hooks, tubercles, thorns, or spines in the last three pairs of the pereopods of some genera suggests the family to be polyphyletic (Błażewicz-Paszkowycz, 2007a). Typhlotanaidae are also characterized by their strong sexual dimorphism (Sieg, 1986; Błażewicz-Paszkowycz et al., 2014). Typhlotanuid females live in self-constructed tubes (Johnson and Attramadal, 1982), but sexually mature ‘swimming’ males show a hydrodynamic appearance with short pereonites and well-developed pleopods (Sieg, 1984; Błażewicz-Paszkowycz et al., 2014). Despite that males of deep-sea Paratanaoidea have never been observed in their natural environment, their body habitus, lack of clinging apparatus, reduced mouthparts, and numerous aesthetascs on the antennules suggest they are short-lived efficient swimmers (Błażewicz-Paszkowycz et al., 2014). Extreme sexual dimorphism prevents the morphological assignment of typhlotanuid males to a particular species, and this can only be solved with certainty through DNA analyses (Błażewicz-Paszkowycz et al., 2014).

Błażewicz-Paszkowycz (2007a) proposed affinities among all known typhlotanuid taxa based on morphological traits (see her

Key for Typhlotanaidae genera and morpho-groups; Błażewicz-Paszkowycz, 2007a), but evolutionary relationships among genera or species remain unknown. Up to six ‘species groups’ were defined by Błażewicz-Paszkowycz (2007a) within *Typhlotanais* sensu lato, including taxa with different morphologies (short or long bodies, pereonites of different shapes, presence/absence of prickly tubercles on carpus, etc.). Nevertheless, morphological studies of this family are particularly difficult, and several taxa remain unassigned to a species group and relationships among groups still remain unsolved. Genetic data for the Typhlotanaidae family are scarce in public databases though, with less than 30 sequences currently available in GenBank (accessed on 17 June 2022) and half of those belonging to just a couple of species (i.e., *Typhlotanais variabilis* and *Pulcherella pulcher*). There is a need for further genetic studies to clarify relationships between genera and to test the validity of previous hypotheses, based on morphological data only.

The main objective of this study is to improve our knowledge on deep-sea Typhlotanaidae diversity from the NW Pacific, currently represented by seven genera (Table 1). New species collected from the Kuril-Kamchatka Trench area during the KuramBio and KuramBio II German–Russian expeditions are described and compared with taxa previously reported from the area. An integrative approach, combining molecular and morphological data, is used to identify affinities among typhlotanuid taxa and, whenever possible, link male and female forms of the same species. A preliminary phylogenetic tree is obtained, and relationships among different groups is discussed based on the congruency of molecular and morphological evidence. Finally, an updated identification key for Typhlotanaidae genera and species present in the NW Pacific is provided.

## Materials and methods

### Sampling

A total of 294 typhlotanuid specimens were collected in the Kuril-Kamchatka Trench area (Brandt et al., 2013; Brandt et al., 2016). Sampling was conducted from July to September 2012 and from August to September 2016 during the two German–Russian expeditions KuramBio and KuramBio II (Kuril-Kamchatka Biodiversity Studies), respectively, aboard RV *Sonne* (cruises: SO 223, SO 250) (Brandt et al., 2013; Brandt et al., 2016). Samples were obtained using an epibenthic sledge and Agassiz trawl between 4,830 and 5,643m depth, and stations are presented in Table 2 and Figure 1. Each sample was elutriated and sieved through a 300- $\mu$ m mesh with cold seawater and fixed in precooled 96% ethanol (Riehl et al., 2014). Samples were frozen and kept at  $-20^{\circ}\text{C}$  until further processing.

TABLE 1 Typhlotanais species reported from the northern Pacific Ocean deep sea, including dubious identifications for taxa originally described from NE Atlantic waters.

Species	Type locality	Depth in type locality [m]	Localities	Depth [m]	Reference
<i>Typhlotanais simplex</i> Kudinova-Pasternak, 1984	NW Pacific: Sea of Japan	1,130	NW Pacific: Sea of Japan	455–1,354	Błażewicz-Paszkwowycz, Bamber & Józwiak 2013
<i>Torquella grandis</i> (Hansen, 1913)	NE Atlantic: S of Iceland	1,265	N Pacific NW Pacific: KKT	6,065 4,895–6,090	Kudinova-Pasternak, 1966 Kudinova-Pasternak, 1970
<i>Typhlamia mucronata</i> (Hansen, 1913)	NE Atlantic: NE of Iceland	1,620	N Pacific NW Pacific: KKT N Pacific: Bering Sea	3,800 4,840–6,710 1,040	Kudinova-Pasternak 1973 Kudinova-Pasternak, 1970 Kudinova-Pasternak 1973
<i>Larsenotanais kamchatikus</i> Błażewicz-Paszkwowycz, 2007b	NW Pacific: Oyashio Current	3,150–3,270	–	–	–
<i>Paratyphlotanais japonicus</i> Kudinova-Pasternak, 1984	NW Pacific: Sea of Japan	3,340–3,350	NW Pacific: Sea of Japan	2,511–3,665	Błażewicz-Paszkwowycz, Bamber & Józwiak 2013
<i>Peraeospinosus brachyurus</i> (Beddard, 1886)	Central Pacific	3,750	–	–	–
<i>Peraeospinosus magnificus</i> (Kudinova-Pasternak, 1970)	NW Pacific: KKT	4,895	N Pacific	3,610	Kudinova-Pasternak 1973
<i>Typhlotanais longicephala</i> Kudinova-Pasternak, 1970	NW Pacific: KKT	4,895	–	–	–
<i>Meromonakantha setosa</i> (Kudinova-Pasternak, 1966)	Central Pacific	6,050	NW Pacific: KKT	4,895	Kudinova-Pasternak, 1970
<i>Peraeospinosus rectus</i> (Kudinova-Pasternak, 1966)	Central Pacific	6,065	NW Pacific: KKT N Pacific NW Pacific Central Pacific Central Pacific	4,895 3,610 7,370 6,400 6,330	Kudinova-Pasternak, 1970 Kudinova-Pasternak 1973 Kudinova-Pasternak 1976 Kudinova-Pasternak 1976 Kudinova-Pasternak 1978
<i>Torquella angularis</i> (Kudinova-Pasternak, 1966)	Central Pacific	6,065	NW Pacific	5,473	Błażewicz-Paszkwowycz 2007b
<i>Typhlotanais compactus</i> Kudinova-Pasternak, 1966	Central Pacific	6,065	NW Pacific: KKT N Pacific NW Pacific	4,895–6,090 1,550–4,260 3,272–5,473	Kudinova-Pasternak, 1970 Kudinova-Pasternak 1973 Błażewicz-Paszkwowycz 2007b
<i>Typhlotanais kussakini</i> Kudinova-Pasternak, 1970	NW Pacific: KKT	6,090–6,135	–	–	–
<i>Torquella elegans</i> (Kudinova-Pasternak 1978)	NW Pacific: W of Philippines	6,330	–	–	–

Environmental data and chemical composition for the sediment of each station were obtained from previous KuramBio reports (Brandt and Maljutina, 2015; Sattarova and Artemova, 2015; Brandt et al., 2016; Kolesnik et al., 2019). Abiotic parameters obtained during the KuramBio and II expeditions were extracted from the original reports and include temperature (°C), bottom current (cm/s), and oxygen concentration (mM/L). Chemical parameters analyzed include organic carbon and several microelements (Si, Al, Fe, Mn, Ca, K, Mg, Ti, Li, Ba, Co, Cu, Cs, Ni, Mo, Pb, Rb, Th, U, Sr, Zn) (Brandt et al., 2013; Sattarova and Artemova, 2015). Species abundance estimates were correlated with each variable using the Spearman non-parametric correlation test as implemented in Mathematica v.12.1 (Wolfram Research Inc, 2020). Cumulative curves of abundance increase with depth were built using the FoldList function in Mathematica v.12.1 (Wolfram Research Inc, 2020).

The factor analysis was carried out in R Studio version 4.0.4, following the instructions at <https://www.geo.fu-berlin.de/en/v/soga/Geodata-analysis/factor-analysis/A-simple-example-of-FA/index.html>.

## Morphological analyses

Initial species identification based on morphological observations was carried out with a dissecting microscope (Nikon Eclipse 50i). Selected individuals were dissected with chemically sharpened tungsten needles, and dissected cephalothorax, pereon, and pleon appendages were mounted on slides using glycerin. Morphological drawings were prepared using a light microscope equipped with a *camera lucida*. Digital drawings were completed using a graphic tablet following

TABLE 2 Stations where Typhlotanidae were found during the KuramBio and KuramBio II expedition.

Expedition	Station	Longitude	Latitude	Depth [m]	Temperature [°C]	Oxygen (µM/l)	Current [cm/s]	Date
KuramBio	1-10	43°57.92'N	157°23.76'E	5,423–5,429	1.6 ± 0.001	155.3 ± 0.3	7.4 ± 1.8	30 July 2012
	1-11	43°58.10'N	157°24.06'E	5,412–5,418	1.6 ± 0.001	154.7 ± 0.2	4.3 ± 1.6	30 July 2012
	2-9	46°11.08'N	155°35.22'E	4,830–4,863	1.5 ± 0.001	156.7 ± 0.3	5.9 ± 2.6	2–3 August 2012
	2-10	46°10.99'N	155°35.26'E	4,859–4,863	1.5 ± 0.001	156.7 ± 0.3	8 ± 4.8	03 August 2012
	3-9	47°11.47'N	154°38.63'E	4,987–4,991	1.5 ± 0.001	160.1 ± 0.2	2.1 ± 1.2	08 August 2012
	5-10	43°38.62'N	153°56.97'E	5,375–5,378	1.6 ± 0.001	155.4 ± 0.3	3.8 ± 1.7	11 August 2012
	6-11	42°32.62'N	154°1.12'E	5,291–5,305	1.6 ± 0.001	155.8 ± 0.3	6.2 ± 6.5	15 August 2012
	6-12	42°32.68'N	154°1.27'E	5,304–5,307	1.5 ± 0.001	155.7 ± 0.3	4.4 ± 3.2	15 August 2012
	7-9	43°5.52'N	153°1.54'E	5,216–5,223	1.5 ± 0.001	157.8 ± 0.3	2.3 ± 1.2	17 August 2012
	7-10	43°1.65'N	152°58.45'E	5,218–5,221	1.5 ± 0.001	157.8 ± 0.3	4 ± 2.5	17 August 2012
	8-9	42°15.82'N	151°48.20'E	5,125–5,140	1.5 ± 0.001	157.5 ± 0.2	3.3 ± 1.3	20 August 2012
	8-12	42°15.75'N	151°48.12'E	5,088–5,130	1.5 ± 0.001	157.5 ± 0.2	3.3 ± 1.3	21 August 2012
	9-9	40°38.79'N	150°59.97'E	5,399–5,408	1.6 ± 0.001	158.3 ± 0.3	3.3 ± 3.2	23 August 2012
	9-12	40°38.71'N	150°59.72'E	5,392–5,397	1.6 ± 0.001	158 ± 0.3	2.3 ± 1.7	24 August 2012
	10-9	41°15.66'N	150°5.70'E	5,265–5,643	1.5 ± 0.001	156.2 ± 0.4	5.5 ± 2.6	26 August 2012
	10-12	41°8.44'N	150°5.53'E	5,249–5,262	1.5 ± 0.001	156.4 ± 0.5	3.7 ± 2	27 August 2012
	11-9	40°16.03'N	148°8.71'E	5,362–5,362	1.5 ± 0.001	157.6 ± 0.6	12.4 ± 18.8	30 August 2012
	11-12	40°15.84'N	148°8.90'E	5,348–5,351	1.5 ± 0.001	158.1 ± 0.8	11.2 ± 9.9	31 August 2012
12-4	39°46.72'N	147°11.90'E	5,215–5,228	1.5 ± 0.002	160.3 ± 0.6	5 ± 2.8	31 August 2012	
KuramBio II	8	43°51.698'N	151°45.85'E	5,103–5,109	NA	NA	NA	19 August 2016
	10	43°51.810'N	151°46.54'E	5,103–5,188	NA	NA	NA	19 August 2016
	86	44°56.784'N	151°6.009'E	5,534–5,630	NA	NA	NA	16 September 2016
	87	44°58.024'N	151°5.589'E	5,640–5,465	NA	NA	NA	16 September 2016

NA, data not available.

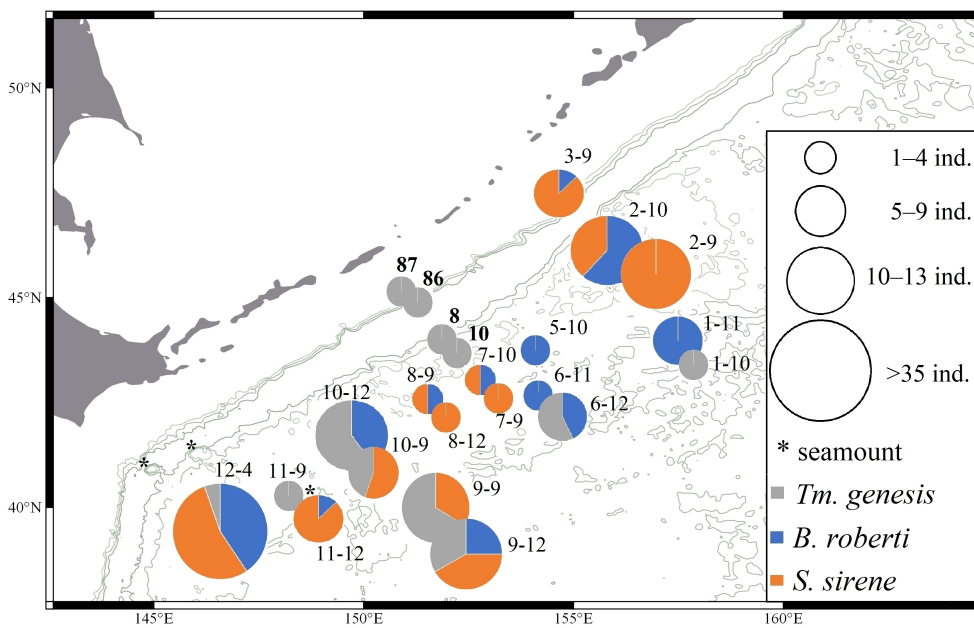


FIGURE 1

Distribution of *Typhlamia genesis* n. sp. (gray), *Baratheonus roberti* n. sp. (blue), and *Starkus sirene* n. sp. (orange) across stations from KuramBio and KuramBio II (in bold). Pie charts represent the relative frequency of each species and their size indicates the sample size per station.

Coleman (2003); Frutos, 2022. Total body length (TBL) was measured along the central axis of symmetry from the frontal margin to the telson's end; body width (BW) was measured perpendicular to the symmetry axis at the widest point along the central axis. The width and length of carapace, pereonites, pleonites, and pleotelson were measured on whole specimens. The measurements were made with a camera connected to the microscope (Nikon Eclipse Ci-L) and the NIS-Elements View software ([www.nikoninstruments.com](http://www.nikoninstruments.com)). Specimen morphology might be slightly distorted due to sampling and ethanol fixation, but it is assumed here that this does not affect the ratios (L:W) of individual appendages or the morphological traits described (number and types of setae/spines).

Unspecified setae in taxonomic descriptions will refer to simple setae by default. Besides simple setae (= without ornamentation), four other types were recognized: (1) serrated—with serration or denticulation, (2) plumose—with delicate setulae tufts distributed along the central axis, (3) penicillate—with a distal tuft of setules and supracuticular articulation, and (4) rod—distally inflated and with a pore (Thomas, 1970; Garm, 2004). Chemosensory setae, which are truncated and have a hollow located distally or subdistally (rod), are highlighted in the figures with an asterisk (\*). According to Segadilha et al. (2018), the cusps on the edge of the maxilliped endites in Typhlotanidae are always articulated structures (contrary to Bird and Larsen, 2009) and often have a distal pore, which might suggest a chemosensory function (Obenchain and Galun, 1982). The 'comb-like' scales present on antennules, antennae, and chelipeds are homologous to the so-called microtrichia from previous Tanaidacea studies (Bird, 2004; Błażewicz-Paszkowycz, 2007a). The term 'clinging apparatus' (= prickly tubercles) refers to a system of various hooks, tubercles, thorns, and spines, located on the carpus of pereopods 4–6 (Błażewicz-Paszkowycz, 2007a; Gellert et al., 2022). The distal part of the cheliped basis, extending backward, is referred to here as 'cheliped lobe' (Larsen, 2005). The term 'collar' is used to refer to the pereonite-1 shape, with a deeply concave anterior edge and lateral corners extended forward. The 'collar' form relates to representatives of the genus *Torquella* and *Ty. variabilis*. Błażewicz-Paszkowycz (2007a) proposed a classification of typhlotanids into two forms—'short-bodied' (body <6.0 L:W) and 'long-bodied' (body ≥8.0 L:W) (see Błażewicz-Paszkowycz, 2007a Key for Typhlotanidae genera and morpho-groups).

Specimens are assigned to the following developmental stages: juvenile, neuter, adult male, and female. Brooding females are defined by the presence of a marsupium with fully developed oostegites. Males are dimorphic and come in two forms: preparatory (juvenile) and swimming male (adult). The neuter is the post-manca stage, which cannot be classified as male or female. Juveniles comprise manca-2 stages, with undeveloped pereonite-6 and lacking pereopod-6, and manca-3 stages, with developed pereonite-6 but undeveloped pereopod-6, and often absent or

reduced pleopods. Abbreviations have been used to distinguish between genera: *Ta.* = *Targaryenella*, *Tq.* = *Torquella*, *Tm.* = *Typhlamia*, *Ty.* = *Typhlotanais*, and *To.* = *Typhlotanoides*. The type material for the species described here is deposited in Museum der Natur Hamburg, Germany (ZMHK), and ICUL/ITan numbers correspond to unique identifiers from the Invertebrates Collection held at the University of Lodz, Poland.

## DNA analyses

Given the poor condition of several specimens, a final set of 157 individuals were used for molecular study and morphological descriptions. Extraction of DNA from morphologically identified female and unidentified male specimens was performed using the Chelex (InstaGene Matrix, Bio-Rad) method as in Jakiel et al. (2020). Specimen vouchers were recovered after extraction whenever possible. The standard DNA barcoding mitochondrial cytochrome oxidase I (COI) region and the nuclear 18S rRNA region were PCR amplified using the primer pairs polyLCO/polyHCO (5'-GAT TAT WTT CAA CAA ATC ARA AAG ATA TTG G-3' and 5'-TAM ACT TTC WGG GTG ACC AAA RAA TCA-3') (Carr et al., 2011) and 18S 4F/2R (5'-CCA AGG AAG RCA GCA GGC ACG-3' and 5'-GAG TCC CGT GTT GAG TCA ATT AAG C-3') (Pitz and Sierwald, 2010). The reaction protocol for COI consisted of an initial denaturation at 95°C for 3 min, 34× reaction cycles of 95°C for 30 s, 48°C for 30 s, and 72°C for 45 s, and a final extension at 72°C for 5 min, and for 18S rRNA an initial extension at 95°C for 2 min, 35× reaction cycles of 95°C for 1 min, 53.6°C for 45 s, and 72°C for 3 min, and a final extension at 72°C for 10 min. For molecular phylogeny, after Sanger sequencing (Macrogen, Netherlands, Amsterdam), consensus sequences were built using Geneious v9.1.3 ([www.geneious.com](http://www.geneious.com)) and compared with the GenBank database using BLAST (Altschul et al., 1990) to discard contamination from non-arthropod sources. Besides typhlotanids, the closest BLAST hits obtained from GenBank consisted of sequences belonging to the families Akanthophoreidae and Paranarthurellidae, and those were chosen as outgroups.

Our newly obtained sequences and the closest BLAST hits obtained from GenBank were aligned using MAFFT and the L-INSi alignment option (Katoh and Standley, 2013). To improve reliability, we extracted conserved (ungapped) blocks of sequences from the alignment using the Gblocks server with default settings (Castresana, 2000; Talavera and Castresana, 2007; Palero et al., 2008). Nucleotide substitution model selection was performed according to the BIC criterion for each gene partition as implemented in MEGA X (Kumar et al., 2018). The concatenated alignment and selected evolutionary models were used to estimate genetic distances and the corresponding Maximum Likelihood phylogenetic tree in MEGA. Initial trees for the heuristic search were obtained

automatically by applying the neighbor-joining algorithm to a matrix of pairwise distances estimated using the maximum composite likelihood (MCL) approach, then selecting the topology with a superior log-likelihood value. Nodal support was assessed using 500 bootstrap replicates.

## High-resolution imaging

Scanning electron microscopy (SEM) was used to illustrate tiny cuticular structures such as ‘scales’ (Garm, 2004) and a clinging apparatus. SEM imaging was performed using a Phenom ProX scanning electron microscope at the Department of Invertebrate Zoology and Hydrobiology, University of Lodz, Poland, using an air-dryer without a sputter metallic layer (Rewicz et al., 2017).

Confocal laser scanning microscopy (CLSM) images were obtained using an LSM 780 (Zeiss) microscope equipped with a Plan Apochromat 63×/1.4 objective and the InTune tuneable excitation laser system (set to excitation wavelength 555 nm). Specimens were stained for 24 h with an equal-volume mixture of saturated water solutions of Congo Red and acid fuchsin. Before dissection and mounting in 100% glycerol, stained animals were washed thoroughly with 50% aqueous glycerol solution. Fluorescence was registered in a single emission channel (561–695 nm). Images were recorded as Z-stacks with 12.6-ms pixel dwell and two-times line averaging with an optical cross section of 0.5 mm. Collected data were pseudo-colored in gold and reconstructed into a 3D image stack by maximum intensity projection using ZEN software (Zeiss, Germany).

## Results

### Taxonomy

#### Family Typhlotanaidae Sieg, 1984

##### Diagnosis (after Bird and Larsen, 2009)

Eyes or eyelobes lacking. Antennule with three articles. Antenna with six articles. Mandible molar broad, margin nodulose. Maxilliped endite distal margin with two non-articulated processes or cusps. Cheliped basis attached with small sclerite, partly covered by edge of carapace. Marsupium with four pairs of oostegites. Pereopods 1–3 with coxa. Pereopods 4–6 without coxa; carpus with clinging apparatus (=prickly tubercles) with spiniform processes and/or hooks; propodus with one (pereopods 4–5) or three (pereopod-6) dorsodistal setae; dactylus and unguis claw-like. Uropod rami with one or two articles.

##### Genera included

*Antiplotanais* Bamber, 2008; *Aremus* Segadilha et al., 2018; *Larsenotana* Błażewicz-Paszkowycz, 2007a; *Meromonakantha*

Sieg, 1986; *Obesutanais* Larsen, Błażewicz-Paszkowycz and Cunha, 2006; *Paratyphlotanais* Kudinova-Pasternak and Pasternak, 1978; *Peraeospinosus* Sieg, 1986; *Pulcherella* Błażewicz-Paszkowycz, 2007a; *Targarynella* Błażewicz and Segadilha, 2019; *Torquella* Błażewicz-Paszkowycz, 2007a; *Typhlamia* Błażewicz-Paszkowycz, 2007a; *Typhlotanais* Sars, 1882; *Typhlotanoides* Sieg, 1983; *Baratheonus* n. gen., and *Starkus* n. gen.

#### Genus *Typhlamia* Błażewicz-Paszkowycz, 2007 Diagnosis (\*amended from Błażewicz-Paszkowycz, 2007a)

Body elongate, about 8.0 L:W. Carapace about as wide as long, tapering proximally, margins gently rounded. Pereonite margins rounded. Antennule twice as long as carapace; article-1 >6.0 L:W (occasionally with suture in the middle of article); article-3 slender and elongated, about 10 L:W, with distal setae as long as the whole appendage. Maxilliped basis with seta reaching beyond endites. Cheliped basis ventrally separated from pereonite-1 by a gap: merus and carpus ventral setae long (longer than merus distal margin). Pereopods 1–3 coxa without spur; pereopod-1 carpus with long dorsodistal seta; pereopods 4–6 carpus with two rounded/blunt cusps instead of prickly tubercles; unguis tip bifid. Pleopod rami with a gap between most proximal seta and other setae. Uropod long and slender (endopod about 10 L:W); endopod with two articles of subequal length; exopod with one article subequal to endopod proximal article.

##### Type species

*Typhlamia bella* Błażewicz-Paszkowycz, 2007a, by designation.

##### Species included

*Typhlamia bella* Błażewicz-Paszkowycz, 2007a; *Tm. mucronata* (Hansen, 1913); *Tm. sandersi* (Kudinova-Pasternak, 1985) *sensu* Błażewicz-Paszkowycz, 2007a; *Typhlamia genesis* n. sp.

##### Remarks

*Typhlamia* was erected by Błażewicz-Paszkowycz (2007a) to accommodate two species with elongated body, rounded pereonite margins, remarkably extended antennule article-3 (about 10 L:W), long seta on maxilliped basis and pereopod carpus, and unarticled uropodal exopod. *Tm. mucronata* was redescribed by Błażewicz-Paszkowycz (2007a) based on historical material from HMS *Ingolf* cruise Hansen’s collection (syntypes: CRU 3916, CRU 7423, CRU 3885), held in the Natural History Museum of Copenhagen (ZMUC). The genus includes *Tm. bella* from Antarctic waters (Błażewicz-Paszkowycz, 2007a) and *Tm. sandersi* mentioned and drawn by Kudinova-Pasternak (1985): 52, 53) is considered doubtful and represents new genus (Gellert et al., in press). Morphological

differences between those species and the new *Typhlamia* species from NW Pacific are highlighted in [Appendix 1](#).

### *Typhlamia genesis* n. sp.

LSID urn: lsid:zoobank.org:act:3D658815-3C53-464A-BD22-C4E89B894FFB

([Figures 2–4](#))

#### Material examined

Holotype, St. 8, neuter 1.9 mm (ZMHK-62918).

Paratypes: St. 10-9, neuter 3.2 mm (ZMHK-62919, illustrated); St. 1-10, neuter 1.2 mm (ZMHK-62920); St. 6-12, three neuters: 3.0 mm (ZMHK-62921); specimen dissected on slides (ZMHK-62922); specimen broken (ZMHK-62923); St. 9-9, four neuters: 1.6 mm (ZMHK-62924), 1.7 mm (ZMHK-62925), 2.1 mm (ZMHK-62926), 2.4 mm (ZMHK-62927); St. 10-9, two damaged neuters (ZMHK-62928, ZMHK-62929); St. 9-12, two neuters: 2.5 mm (ZMHK-62930), broken specimen (ZMHK-62931); St. 10-12, four neuters: 1.5 mm (ZMHK-62932), 1.5 mm (ZMHK-62933), 1.9 mm (ZMHK-62934), one broken (ZMHK-62935); St. 12-4, two neuters broken (ZMHK-62936; ZMHK-62937); St. 8, two neuters: 2.4 mm (ZMHK-62938), broken individual dissected on slides (ZMHK-62939); St. 10, neuter 3.8 mm (ZMHK-62940, illustrated); St. 10, two neuters: 1.9 mm (ZMHK-62941, illustrated), broken specimen (ZMHK-62941); St. 86, neuter broken (ZMHK-62942); St. 86, neuter 1.9 mm (ZMHK-62943, broken); St. 86, manca-3 2.2 mm (ZMHK-62944); St. 87, neuter broken (ZMHK-62945).

#### Other material examined

St. 9-9, two broken specimens (ICUL7960\*; ICUL4271\*); St. 10-9, neuter 3.1 mm (ICUL7916\*); St. 9-12, two neuters 3.1 mm (ICUL4273\*); 3.25 mm (ICUL4278\*); St. 10-12, neuter (ICUL7915\*); St. 9-9, neuter (ICUL7956\*); St. 11-9, neuter (ICUL7968\*); St. 6-12, neuter (ICUL7914\*).

\*Individual not recovered after DNA extraction.

#### Diagnosis

Pereopod-1 propodus with ventrodiscal seta. Pereopod-2 merus with ventrodiscal seta. Pereopod-2 carpus with two long setae. Pereopods 4–6 ischium with two setae. Uropod exopod subequal to endopod proximal article.

#### Etymology

The generic name *Typhlamia* is linked with the record ‘The Lamia’ from the album The Lamb Lies Down on Broadway from the music band Genesis. Name of species after the Genesis music band.

#### Description of neuter

TBL 3.0 mm. Paratype. Body ([Figures 2A–C](#)) slender, 7.5 L:W. Cephalothorax with short and rounded rostrum, 1.0 L:W, 1.2×

pereonite-1, naked; eyes absent. Pereonites 1–6: 0.8, 1.0, 0.9, 1.0, 0.8, and 0.7 L:W, respectively. Pereonite-1 trapezoidal, 0.6× pereonite-2; pereonite-2 hexagonal, 1.2× pereonite-3; pereonite-3 hexagonal, 0.9× pereonite-4; pereonite-4 trapezoidal, 1.3× pereonite-5; pereonite-5 trapezoidal, 1.1× pereonite-6; pereonite-6 trapezoidal. Pleon 0.2× TBL; pleonites 1–5: all the same size—0.2 L: W. Pleotelson 2.1× pereonite-6.

Antennule ([Figure 3A](#)) 1.9× cephalothorax; article-1 5.5 L:W, 0.5× antennule total length, with five (two penicillate medial) setae, two (one penicillate distal) setae, and with some scales proximally; article-2, 4.8 L:W, 0.3× article-1, with two distal setae; article-3, 16 L:W, 2.0× article-2, with one penicillate and six long distal setae.

Antenna ([Figure 3B](#)) of six articles; article-1 fused with body; article-2, 1.3 L:W, with short seta; article-3, 1.3 L:W, 0.7× article-2, with short ventral seta; article-4, 6.7 L:W, 4.0× article-3, with six (three penicillate distal setae) setae; article-5, 7.3 L:W, 0.6× article-4, with long seta; article-6 1.5 L:W, with five long distal setae.

Mouthparts. Labrum ([Figure 3C](#)) hood-shaped, distally naked. Mandible ([Figures 3D, E](#)) molar broad, edges with rounded tubercles; left mandible ([Figure 3D](#)) incisor with three lobes, *lacinia mobilis* well developed, with single lobe; right mandible ([Figure 3E](#)) incisor with three lobes without *lacinia mobilis*. Labium ([Figure 3F](#)) distal part finely setose. Maxillule ([Figure 3G](#)) endite with eight terminal spines, two innermost spines shorter than the others. Maxilla ([Figure 3H](#)) semi-triangular. Maxilliped ([Figure 3I](#)) basis with long, finely serrated seta reaching behind endites; endites unfused, with two small cusps, one seta, and scales on outer margin; palp with four articles: article-1 naked; article-2 wedge, with three serrated inner setae and scales on outer margin (outer seta not seen); article-3 with four serrated inner setae and scales on outer margin; article-4 with six serrated inner distal and outer setae. Epignath not observed.

Cheliped ([Figure 4A](#)) basis slender, naked, 2.1 L:W, lobe separated by a gap from pereonite-1; merus subtriangular, with long ventral seta; carpus 4.1 L:W, with two long ventral setae, dorsal margin with distal chemosensory seta and proximal setae; chela subequal to carpus, 4.8 L:W; palm 0.7× fixed finger, with two rod setae near dactylus insertion (inner and outer surface); fixed finger with two long ventral setae; cutting edge with three setae and three weak, blunt cusps distally; dactylus with short dorsoproximal seta.

Pereopod-1 ([Figure 4B](#)) walking type, overall 26 L:W; coxa with seta; basis 8.6 L:W with subproximal short seta; ischium with ventral seta; merus 3.5 L:W with ventrodiscal seta; carpus 3.6 L:W, 1.1× merus, with five (one chemosensory distal) setae; propodus 6.3 L:W, 1.3× carpus, with one dorsodistal and one ventrodiscal setae; dactylus 0.7× unguis, with subproximal seta; dactylus and unguis together 0.9× propodus; unguis simple.

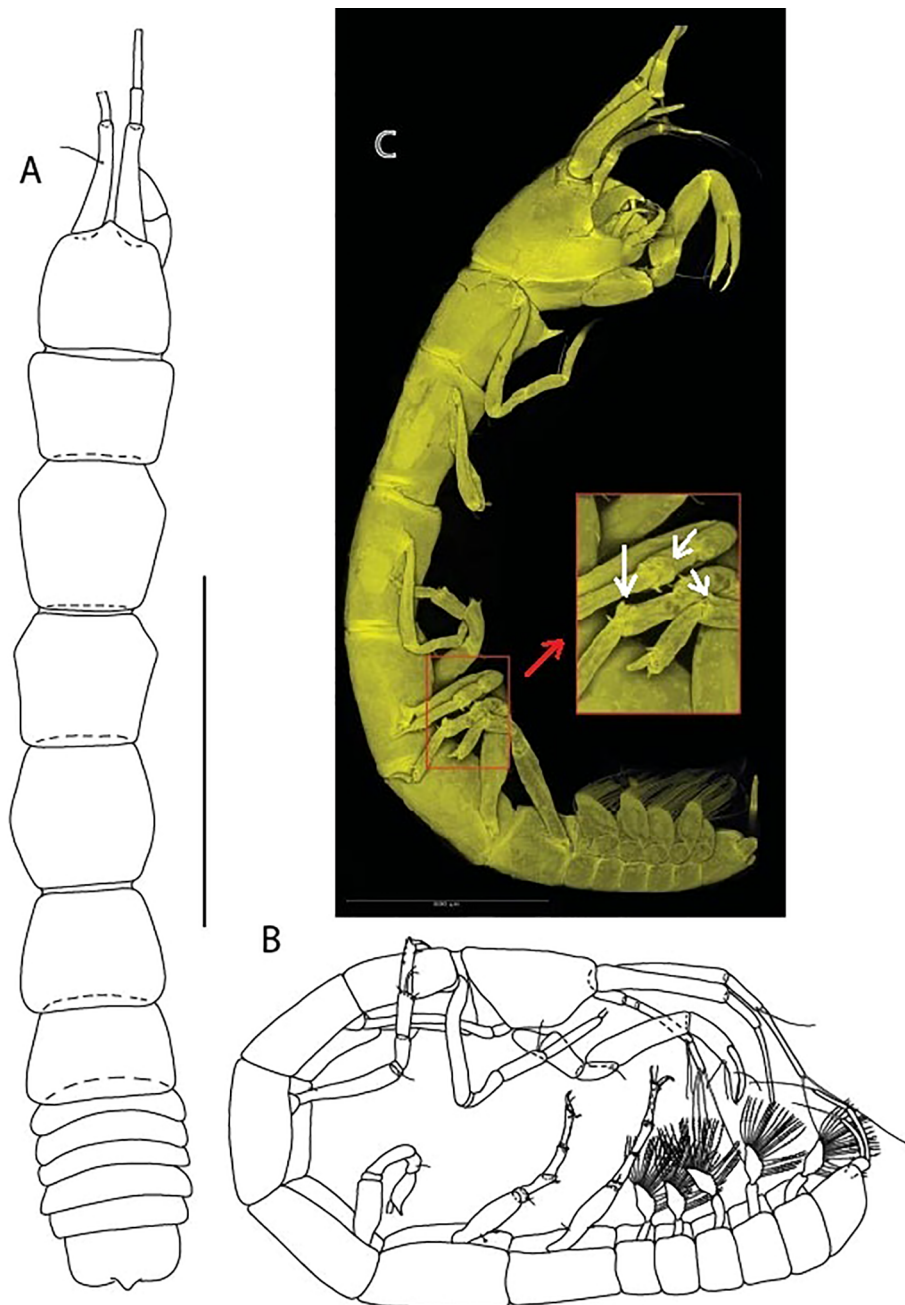


**FIGURE 2**  
*Typhlamia genesis* n. sp., neuter: (A) Body, dorsal view (ZMHK-62919); (B) Body, lateral view (ZMHK-62941). (C) CLSM images (ZMHK-62918): *Tm. genesis* pereopods 4–6 carpi with two cusps. Scale: A–B = 1 mm, C = 0.5 mm.

Pereopod-2 (Figure 4C) walking type; coxa with seta; basis naked; ischium with ventral seta; merus 2.4 L:W, with ventrodorsal seta; carpus 3.2 L:W, 1.3× merus, with two distal spines, two long (longer than half of propodus) and one short setae; propodus 4.7 L:W, 1.4× merus and carpus combined, with two dorsodistal setae (one long) and ventrodorsal spine; dactylus 0.9× unguis; dactylus and unguis together 0.4× propodus; unguis simple.

Pereopod-3 (Figure 4D) walking type, overall 14 L:W; coxa with seta; basis 6.4 L:W, with subproximal dorsal seta; ischium with ventral seta; merus 2.4 L:W, with ventrodorsal seta; carpus 3.6 L:W, 1.5× merus, with spine, two short and two long setae distally; propodus 5.6 L:W, 1.2× carpus, with dorsodistal seta, ventrodorsal spine and numerous scales; dactylus 0.9× unguis; dactylus and unguis together 0.4× propodus; unguis simple.

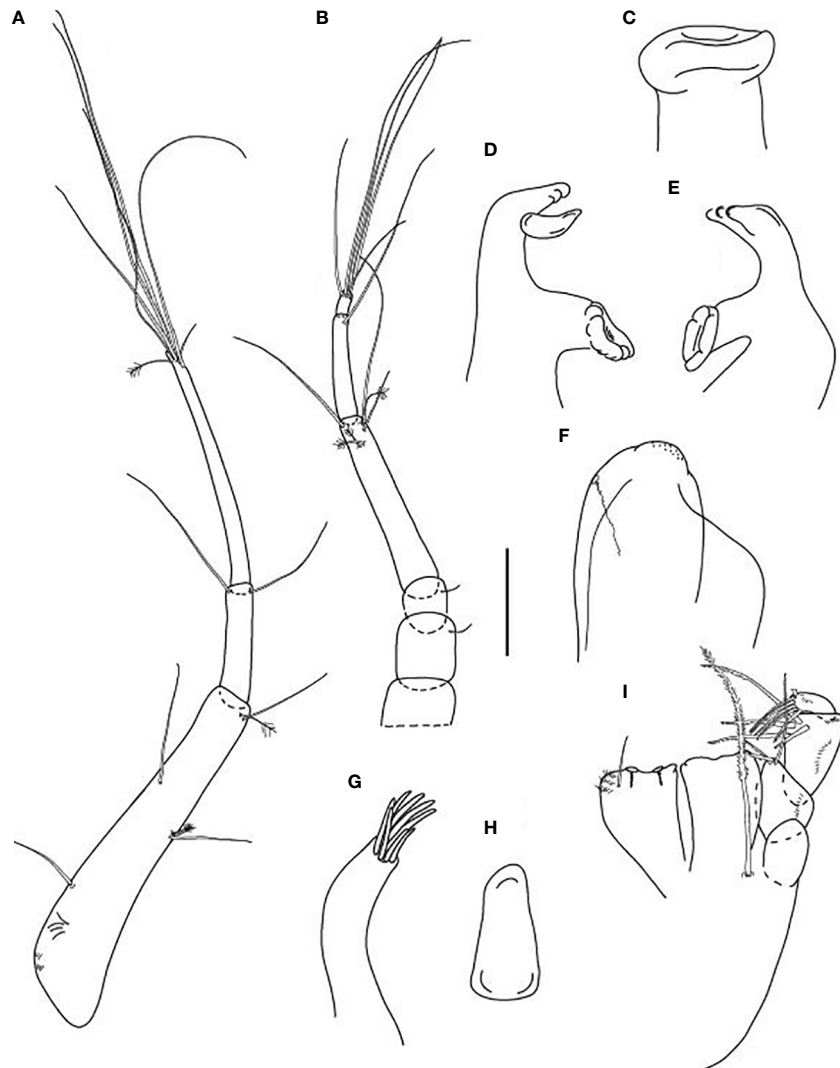


FIGURE 3

*Typhlamia genesis* n. sp., neuter (ZMHK-62922), (A) Antennule; (B) Antenna; (C) Labrum; (D) Left mandible; (E) Right mandible; (F) Labium; (G) Maxillule; (H) Maxilla; (I) Maxilliped. Scale: A–I = 0.1 mm

Pereopod-4 (Figure 4E) clinging type, overall 12 L:W; coxa absent; basis slender, 4.2 L:W, naked; ischium with two ventral setae; merus 3.4 L:W, with spine and seta ventrodistally; carpus 4.2 L:W, 1.2× merus, with two cusps (Figure 2C), two spines and dorsal seta distally; propodus 7.7 L:W, with numerous scales, two dorsodistal seta and ventrodistal spines; dactylus 2.5× unguis, both combined 0.6× propodus; unguis bifurcated.

Pereopod-5 (Figure 4F) as pereopod-4, but basis with two penicillate setae.

Pereopod-6 (Figure 4G) as pereopod-4, but basis with two setae (middorsal and midventral), propodus with three dorsodistal setae.

Pleopods (Figure 4H) basal article naked; exopod with 13 plumose setae on outer margin and one on inner margin; endopod with 21 plumose setae on outer margin.

Uropod (Figure 4I) basal article 1.5 L:W, naked; endopod two-articled, proximal article 0.7× distal article, naked; distal article with penicillate medial and five long terminal setae; exopod one-articled, subequal to endopod article-1, with one medial, one long and one robust terminal setae.

#### Distribution

*Typhlamia genesis* n. sp. is known from seven locations off Kuril-Kamchatka Trench in a depth range of 5103–5643 m (Figure 1).

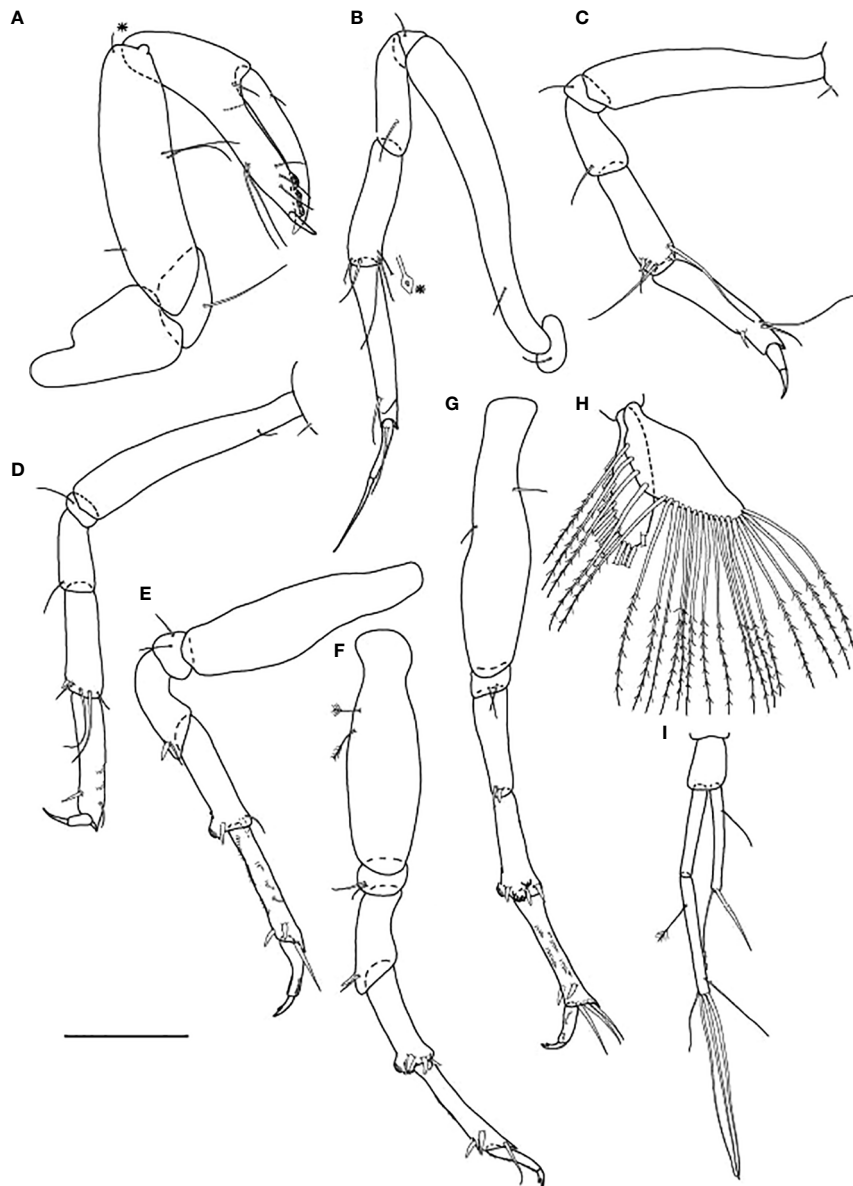


**FIGURE 4**  
*Typhlamia genesis* n. sp., neuter: (A) Cheliped (ZMHK-62939); (B) Pereopod-1 (ZMHK-62939); (C) Pereopod-2 (ZMHK-62939); (D) Pereopod-3 (ZMHK-62939); (E) Pereopod-4 (ZMHK-62922); (F) Pereopod-5 (ZMHK-62922); (G) Pereopod-6 (ZMHK-62922); (H) Pleopods (ZMHK-62922); (I) Uropods (ZMHK-62940). Scale: (A–I) = 0.1 mm.

**Remarks**

*Typhlamia genesis* n. sp. is the first *Typhlamia* species discovered in Pacific. It is distinguished from other members of the genus by the presence of only one seta on merus of pereopods 1–3, while the other species have two setae. Distinguishing features of *Typhlamia* species are summarized in [Appendix 1](#).

**Key for identification of *Typhlamia* females**

1. Uropod exopod longer than endopod proximal article .....*Tm. mucronata* (Hansen, 1913) (N Atlantic; 1618–1847 m)
- Uropod exopod subequal to endopod proximal article.....2
2. Pereopod-1 propodus with two dorsodistal setae

- .....*Tm. sandersi* (Kudinova-Pasternak, 1985)  
(Mid-Atlantic Ridge; 3080–3140 m)
- Pereopod-1 propodus with one dorsodistal seta.....3
3. Pereopod-2 merus with one seta..... *Typhlamia genesis*  
n. sp.  
(NW Pacific; 5215–5643 m)
- Pereopod-2 merus with two setae of unequal length  
.....*Tm. bella* Błażewicz-Paszkowycz, 2007a  
(W Antarctic; 4385–4392 m)

## Genus *Baratheonus* n. gen.

LSID urn:lsid:zoobank.org:act:776C32D6-4005-4889-AAC6-88BF891DE4CF

### Diagnosis

Body elongated (~9.0 L:W). Pereonites with straight margins; pereonite-1 short; pereonites 1–3 smooth (without corrugation or grooves), lateral margins parallel. Pleotelson apex without spines. Antennule, antennae, and cheliped without scale ornamentation. Antennule article-3 regular length (4.0 L:W). Antenna article-2 long (2.5 L:W), without apophyses. Cheliped basal lobe separated from pereonite-1 by a gap. Pereopods 1–3 coxa without spurs; basis without spines; ischium with short seta; propodus with numerous ventral setae. Pereopods 2–3 carpus with four distal setae, propodus with two long ventrodiscal setae. Pereopods 4–6 carpus with large prickly tubercles (longer than half of the carpus length), not surrounded by a row of blunt spines; propodus long (6.0 L:W), with dorsodistal short seta (< half of dactylus length); dactylus 3.0× unguis; unguis simple. Uropodal endopod and exopod one-articled; exopod 0.7× endopod.

### Type species

*Baratheonus roberti*, by monotypy.

**Gender.** Masculine.

**Etymology.** Named after the Baratheon family from George R.R. Martin's novel *Game of Thrones*.

### Remarks

*Baratheonus* n. gen. with body 9.0 L:W represents 'long-bodied' forms of typhlotanoids. The prickly tubercles on carpus of pereopods 4–6 (=clinging apparatus) allow to immediately distinguish it from other typhlotanoids lacking clinging apparatus, e.g., *Meromonakantha*, *Paratyphlotanais*, *Obesutanais*, *Aremus*, and *Targarynella* (Błażewicz-Paszkowycz, 2007a; Segadilha et al., 2019). Parallel margins in smooth pereonites distinguish *Baratheonus* n. gen. from genera with rounded pereonite margins (i.e., *Torquella*, *Peraeospinosus*, and

*Pulcherella*) and from the 'plicatus' group (with corrugated pereonites). One-articled uropodal exopod of *Baratheonus* n. gen. is the character shared with several typhlotanoids like (1) 'greenwichensis' group (*Typhlotanais ischnochela* Segadilha and Serejo, 2022, *Typhlotanais greenwichensis* Shiino, 1970, *Typhlotanais messinensis* G.O. Sars 1882, *Typhlotanais herthio* Błażewicz-Paszkowycz & Bamber, 2012), (2) the 'trispinosus' group (*Typhlotanais trispinosus* Hansen, 1913, *Typhlotanais tenuicornis* Sars, 1882, *Typhlotanais spatulasetosus* Larsen, 2012, *Typhlotanais spinibasis* Segadilha and Serejo, 2022), and (3) ten unclassified *Typhlotanais* species (*Typhlotanais assimilis* Sars, 1882, *Typhlotanais aequiremis* (Lilljeborg, 1864), *Typhlotanais kussakini* Kudinova-Pasternak, 1970, *Typhlotanais guca* Błażewicz-Paszkowycz, Bamber and Cunha, 2011, *Typhlotanais inaequipes* Hansen, 1913, *Typhlotanais longiseta* Segadilha and Serejo, 2022, *Typhlotanais proctagon* Tattersall, 1904, *Typhlotanais profundus* Hansen, 1913, *Typhlotanais plebejus* Hansen, 1913, and *Typhlotanais williamsae* Dojiri and Sieg, 1997). Distinguishing *Baratheonus* n. gen. from the 'greenwichensis' group and 'trispinosus' group is a straightforward procedure, as the new genus lacks the coxal spur on pereopods 1–3 (present in 'greenwichensis' groups) but also lacks the spines on members 2 and 3 of the antenna (present in 'trispinosus'). Furthermore, the large prickly tubercles and simple unguis in pereopods 4–6 separate *Baratheonus* n. gen. from *Ty. aequiremis*, which has relatively small tubercles and bifurcated unguis (Błażewicz-Paszkowycz 2007; Figures 15E, F). The long articles in pereopods 4–6, with very short propodal dorsodistal seta, separates *Baratheonus* n. gen. from *Ty. kussakini* and *Ty. williamsae*. Finally, *Baratheonus* n. gen. has short pereonite-1 (longer in *Ty. williamsae* and *Ty. kussakini*) and unarticulated uropodal rami (two-articled endopod in *Ty. williamsae*). *Baratheonus* n. gen. and *Typhlotanais longiseta* Segadilha and Serejo, 2022, have several ventral setae on pereopods 2–3 (also on pereopod-1 in *Baratheonus* n. gen.). A one-articled uropodal exopod and endopod in *Baratheonus* n. gen. distinguishes it from *Typhlotanais andradeorum* Segadilha and Serejo, 2022, which has two-articled uropodal exopod and endopod. *Typhlotanais assimilis*, *Ty. inaequipes*, *Ty. longiseta*, *Ty. profundus*, and *Ty. plebejus* have two-articled endopod and one-articled exopod. Additionally, *Baratheonus* n. gen. cheliped lobe is separated by a gap from pereonite-1, which *Ty. longiseta* does not have. *Baratheonus* n. gen. has pereopods 2–3 merus with two and three setae, respectively, contrarily to *Ty. guca* and *Ty. proctagon*, which have a large ventrodiscal spine.

### *Baratheonus roberti* n. sp.

LSID urn:lsid:zoobank.org:act:8DFB8FBC-A4F8-4E7A-BEF3-0A7C639027F4  
(Figures 6–7)

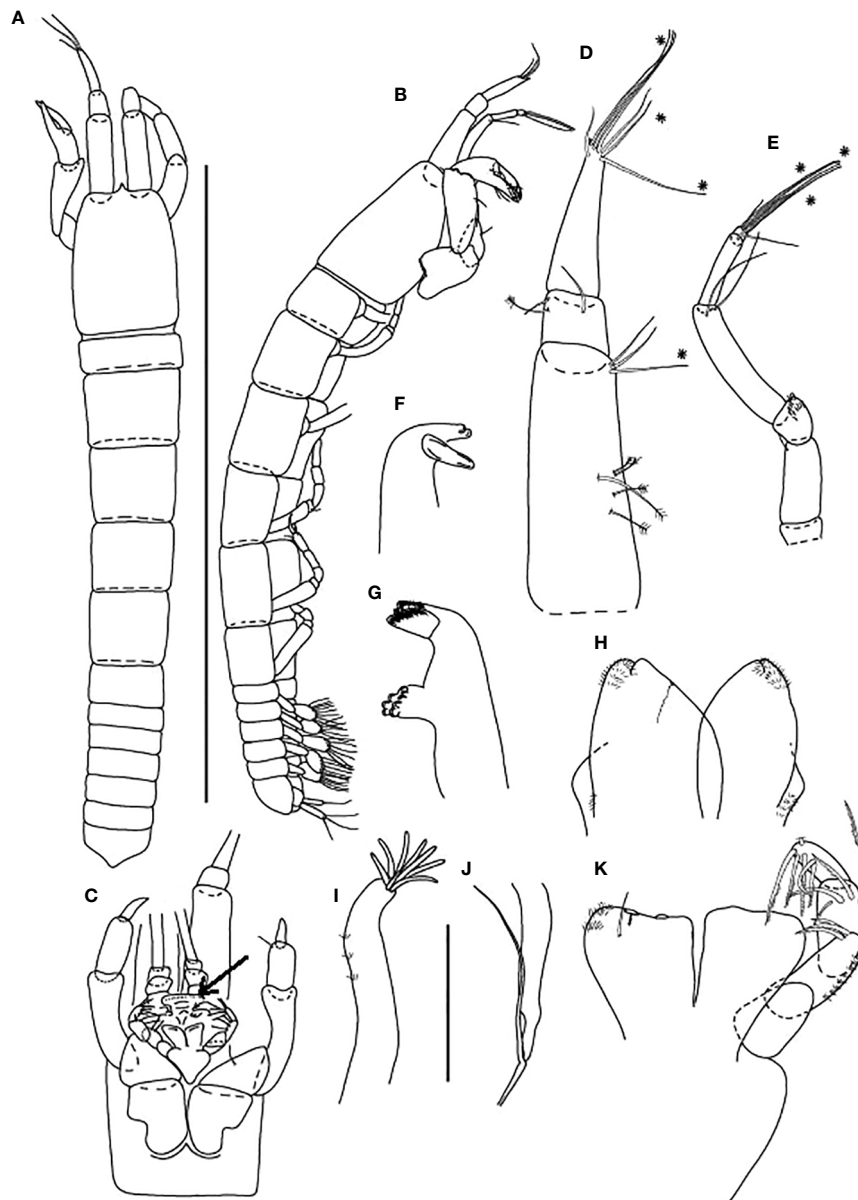


FIGURE 5

*Baratheonus roberti* n. sp., neuter: (A) Body, dorsal view (ZMHK-62895); (B) Body, lateral view (ZMHK-62891); (C) Carapace ventral side (ZMHK-62891); (D) Antennule (ZMHK-62898); (E) Antenna (ZMHK-62898); (F) Left mandible (ZMHK-62908); (G) Right mandible (ZMHK-62908); (H) Labium (ZMHK-62908); (I) Maxillule (ZMHK-62908); (J) Palp (ZMHK-62908); (K) Maxilliped (ZMHK-62908). Scale of body: (A, B) = 1 mm, (D–K) = 0.1 mm.

## Material examined

Holotype, St. 12-4, neuter 1.9 mm (ZMHK-62891, illustrated).

Paratypes, St. 1-11, neuter broken (ZMHK-62892); St. 2-10, five neuters: one 0.7 mm (ZMHK-62893), one 2.0 mm (ZMHK-62894), one individual dissected on slides (ZMHK-62895, broken and illustrated), two individuals broken (ZMHK-62896; ZMHK-62897); St. 6-12, two neuters dissected on slides (ZMHK-62898), individual broken (ZMHK-62899); St. 5-10, neuter 1.2 mm (ZMHK-62900); St. 7-10, neuter broken

(ZMHK-62901); St. 8-9, two neuters 1.7 mm (ZMHK-62902; ZMHK-62909); St. 9-12, neuter broken (ZMHK-62904); St. 10-12, three neuters broken (ZMHK-62905; ZMHK-62906; ZMHK-62907); St. 12-4, neuter 1.3 mm dissected on slides (ZMHK-62908), neuter 1.4 mm (ZMHK-62909), two individuals broken (ZMHK-62910; ZMHK-62911; dissected on slides), five individuals broken (ZMHK-62912; ZMHK-62913; ZMHK-62914; ZMHK-62915; ZMHK-62916), female with oostegites 1.8 mm (ZMHK-62917).

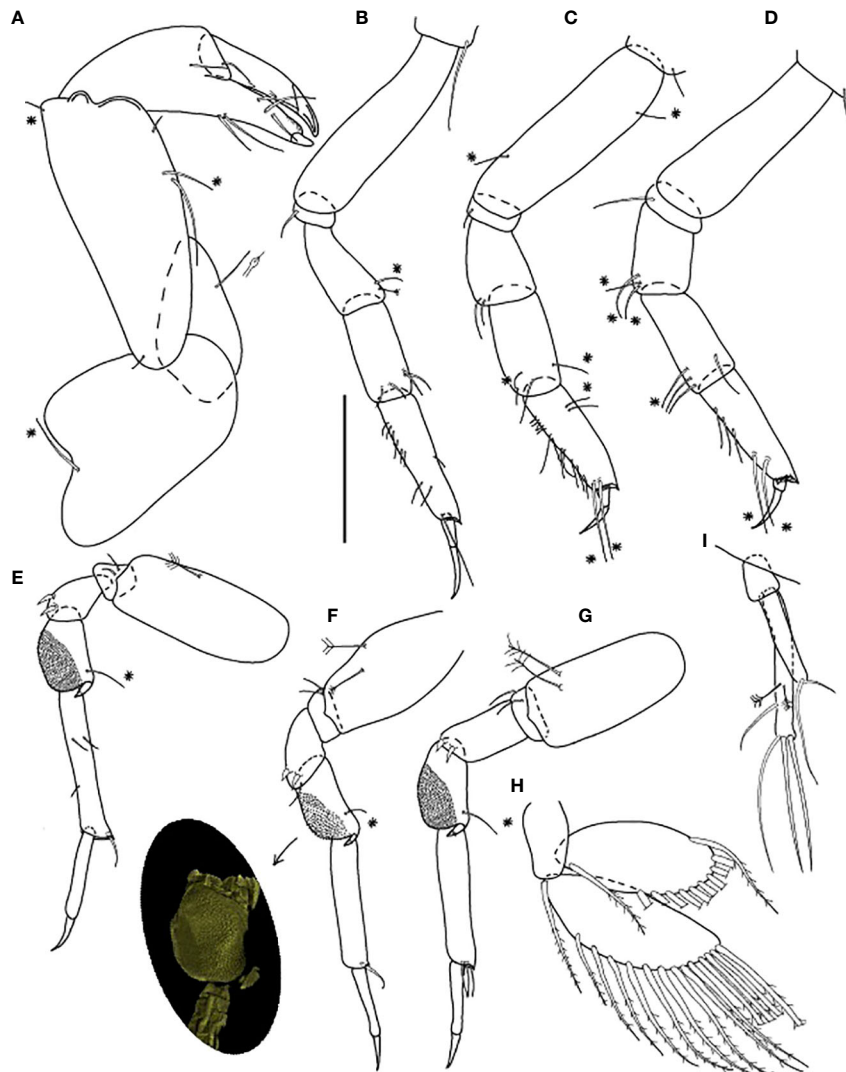


FIGURE 6

*Baratheonus roberti* n. sp., neuter: (A) Cheliped (ZMHK-62898); (B) Pereopod-1 (ZMHK-62899); (C) Pereopod-2 (ZMHK-62899); (D) Pereopod-3 (ZMHK-62899); (E) Pereopod-4 (ZMHK-62898); (F) Pereopod-5 (ZMHK-62898 and CLSM image showing the large prickly tubercles (clinging apparatus) (ZMHK-62898); (G) Pereopod-6 (ZMHK-62899); (H) Pleopods (ZMHK-62908); (I) Uropods (ZMHK-62908). Scale: (A–I) = 0.1 mm.

### Other examined material

St. 2-10, neuter 0.2 mm (ICUL7923\*), individual broken (ICUL7937\*); St. 3-9, neuter broken (ICUL7979\*); St. 6-12, neuter 1.7 mm (ICUL4284\*); St. 5-10, neuter 1.3 mm (ICUL4163\*); St. 6-11, neuter broken (ICUL7936\*); St. 9-12, neuter 1.3 mm (ICUL7935\*); St. 10-12, neuter 1.3 mm (ICUL7928\*); St. 11-12, neuter 1.3 mm (ICUL7981\*); St. 12-4, three neuters (ICUL4285\*, ICUL4288\*, ICUL4290\*); St. 12-4, neuter (ICUL7934\*); St. 2-10, neuter (ICUL4200\*); St. 9-12, neuter (ICUL4193\*); St. 12-4 neuter (ICUL7970\*).

\*Individual not recovered after DNA extraction.

### Diagnosis

As for the genus (by monotypy).

**Etymology.** Species named after the character from the novel by George R.R. Martin's novel *Game of Thrones*—Robert Baratheon, the Lord of the Seven Kingdoms of Westeros and the head of House Baratheon of King's Landing.

**Description** of neuter, length 0.9 mm. Body (Figures 5A, B) slender, 8.1 L:W. Cephalothorax rectangular, with the short and pointy rostrum, 1.4 L:W, 4.6× pereonite-1, naked; eyes absent. Pereonites 1–6: 0.3, 0.9, 1.0, 0.9, 1.0, and 0.6 L:W, respectively. Pereonite-1 rectangular, shortest, 0.4× pereonites-2; pereonite-2 square, as pereonite-3; pereonite-3 square, 1.1× pereonite-4; pereonite-4 square, the same length as pereonite-5; pereonite-5 square, 1.7× pereonite-6; pereonite-6 rectangular. Pleon 0.3×

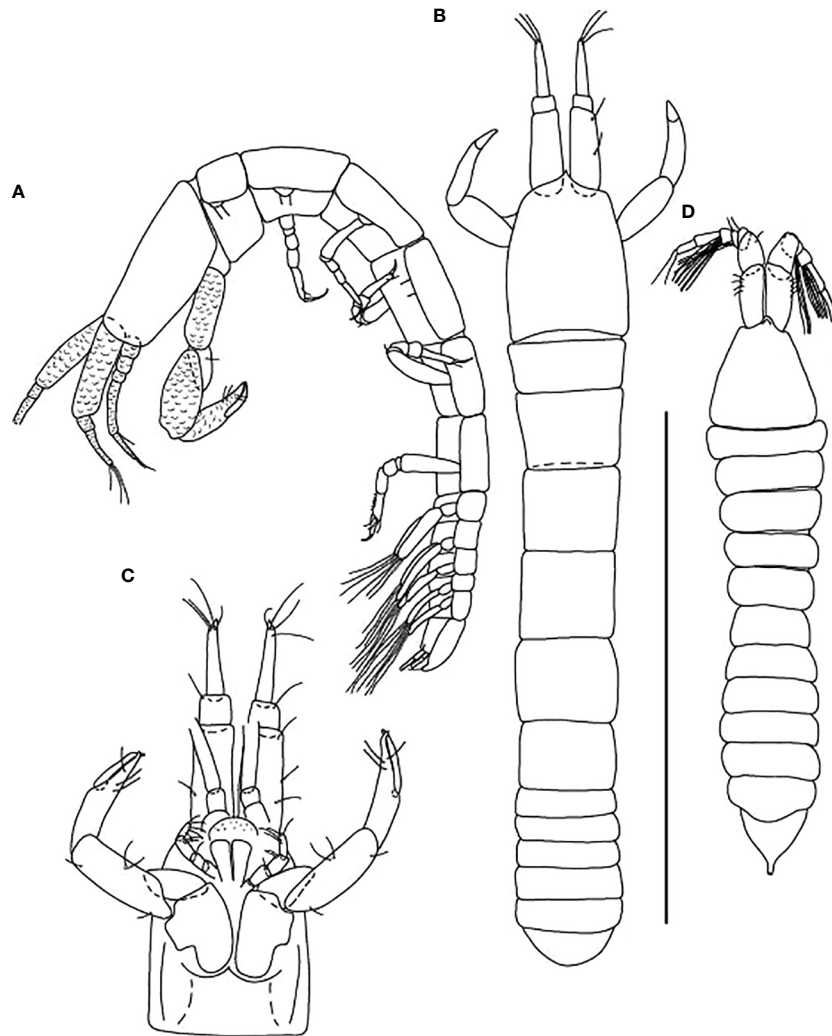


FIGURE 7

*Starkus sirene* n. sp., neuter: (A) Body, lateral view (ZMHK-62865); (B) Body, dorsal view (ZMHK-62875); (C) Carapace ventral side (ZMHK-62875); swimming male: (D) Body, dorsal view (ZMHK-62890). Scale of body: (A–D) = 1 mm.

TBL. Pleonites 1–5: the same size—0.4 L:W. Pleotelson 4.6× pereonite-6.

Antennule (Figure 5D) 0.7× cephalothorax; article-1, 0.6× of antennule total length, 2.5 L:W, with five penicillate medial setae, one chemosensory and two distal setae; article-2, 1.4 L:W, 0.3× article-1, with one penicillate and two distal setae; article-3, 4.0 L:W, 2.0× article-2, with two short, three chemosensory setae distally (truncated with a hollow) and four long setae distally.

Antenna (Figure 5E) of six articles; article-1 short fused with body, naked; article-2 long, 2.5 L:W, with distal seta; article-3, 1.3 L:W, 0.5× article-2, with scales; article-4, 4.4 L:W, 3.1× article-3, with two long distal setae (as long as article-5); article-5, 6.0 L:W, 0.6× article-4, with long distal seta; article-6 minute, with one short, three chemosensory, and three setae distally.

Mouthparts. Labrum (Figure 5C) rounded, distal surface setose. Left mandible (Figure 5F) incisor broken, *lacinia mobilis* well developed, with single lobe; right mandible (Figure 5G) incisor with eight lobes without *lacinia mobilis*. Labium (Figure 5H) with inner lobe distally setose and with scales along margin on the outer lobe. Maxillule (Figure 5I) endite with eight terminal spines (one short) and scales on outer margin; palp (Figure 5J) with two terminal setae. Maxilliped (Figure 5K) endites unfused, with two cusps, distolateral seta, and several scales on outer margin; palp with four articles: article-1 naked; article-2 elongate, with three serrated inner setae and scales on outer margin (outer seta not seen); article-3 with four serrated inner setae; article-4 with five serrated inner setae and one (broken) subdistal outer seta. Epignath not observed.

Cheliped (Figures 5C, 6A) basis 1.7 L:W, with long chemosensory proximal seta; lobe separated by a gap from pereonite-1; merus wedge, with ventral chemosensory seta; carpus 2.6 L:W, with two long medial (one chemosensory) and one short subdistal setae ventrally, and with one distal chemosensory and one proximal dorsal setae; chela 0.9× carpus, 3.1 L:W; palm 1.7× fixed finger, with two setae near dactylus insertion (one on inner surface); fixed finger with two long ventral setae; cutting edge poorly calcified, only gently undulated, with three setae.

Pereopod-1 (Figure 6B) walking type, overall 11 L:W, slender; coxa with long seta, basis 4.1 L:W, naked; ischium with ventral seta; merus 2.2 L:W, with one chemosensory and one penicillate dorsodistal setae; carpus 2.3 L:W, 1.1× merus, with four distal setae; propodus 4.0 L:W, 1.3× carpus, with six short setae on ventral margin, one middorsal short seta, and two ventrodorsal setae; dactylus 0.5× unguis, with subproximal seta; dactylus and unguis together 0.5× propodus; unguis simple.

Pereopod-2 (Figure 6C) walking type, overall 8.0 L:W; coxa with seta; basis 4.4 L:W, with one dorsal and one ventral chemosensory seta; ischium with ventral seta; merus 1.5 L:W, with two ventrodorsal setae; carpus 2.2 L:W, 1.3× merus, with four distal setae (two chemosensory); propodus 3.0 L:W, 0.6× merus and carpus combined, with five short proximal and two subproximal dorsal setae, seven long ventral setae, and two long (longer than unguis) chemosensory ventrodorsal setae; dactylus 0.6× unguis, with subproximal seta; dactylus and unguis together 0.5× propodus; unguis simple.

Pereopod-3 (Figure 6D) walking type, overall 10 L:W; coxa with seta; basis 4.3 L:W, naked; ischium with ventral seta; merus 1.8 L:W, with three chemosensory ventrodorsal setae; carpus 2.2 L:W, 0.8× merus, with one chemosensory and three setae distally; propodus 3.4 L:W, with three ventroproximal setae and two long (longer than unguis) chemosensory ventrodorsal setae, the distal margin with dorsal prolongation and setules; dactylus 0.4× unguis, with subproximal seta; dactylus and unguis together 0.5× propodus; unguis simple.

Pereopod-4 (Figure 6E) clinging type, overall 9.0 L:W; coxa absent; basis robust 2.4 L:W, with penicillate ventral seta; ischium with two ventral setae; merus 1.7 L:W, with two ventrodorsal spines; carpus 1.8 L:W, with large prickly tubercles, distal spiniform apophysis, and chemosensory dorsodistal seta; propodus 5.8 L:W, with three short medial setae and dorsodistal seta (< 0.5× dactylus); dactylus 2.6× unguis, both combined 0.9× propodus; unguis simple.

Pereopod-5 (Figure 6F) as pereopod-4, but basis with two penicillate setae; merus with distal seta; propodus without medial setae.

Pereopod-6 (Figure 6G) as pereopod-4, but basis with two penicillate setae and propodus with three dorsodistal setae.

Pleopod (Figure 6H) basal article naked; exopod with 14 plumose setae on outer margin and one inner seta; endopod with

11 plumose setae on outer margin, gap between most proximal and other setae.

Uropod (Figure 6I) basal article 1.9 L:W; both rami one-articled; exopod 0.6× endopod, with one strong and one small terminal setae; endopod 7.5 L:W, with three medial setae (two penicillate setae) and three terminal setae.

## Distribution

*Baratheonus roberti* n. sp. is known from 12 locations off the Kuril-Kamchatka Trench in a depth range of 4859–5418 m (Figure 1).

## Genus *Starkus* n. gen.

LSID urn:lsid:zoobank.org:act:B996EAF7-20D3-4E0D-A1CD-48D4DAAC3ADD

## Diagnosis

Antennule article-3 long (6.0 L:W), with terminal spur. Carapace narrow, longer than wide. Pereonite-1 shorter than the others, pereonites 2–6 wider than long or square, lateral margins parallel. Cheliped basal lobe separated from pereonite-1 by a gap. Antennule, antennae, and cheliped often with 'scales'. Pereopod-1 articles with setae only; pereopods 2–3 carpus and propodus with ventrodorsal spines; pereopods 4–6 carpus with large, rounded area covered by minute spines (prickly tubercles), dactylus and unguis combined almost as long as propodus, unguis simple. Pleopod rami with proximal seta separated from a gap of the other. Uropod exopod and endopod two-articled.

## Type species:

*Starkus mixtus* (Hansen, 1913).

**Gender:** Masculine.

**Etymology.** The genus name is given after the *Stark* family from George R.R. Martin's novel *Game of Thrones*.

**Species included:** *Starkus mimosis* (Błażewicz-Paszkowycz, 2007a); *S. mixtus* (Hansen, 1913); *S. simplex* (Kudinova-Pasternak, 1984); *Starkus sirene* n. sp.

## Remarks

*Starkus* n. gen. is a genus that can be distinguished from other Typhlotanidae by its two-articled uropod rami and very simple body habitus defined by straight and nearly parallel pereonite lateral margins in dorsal view. Based on just these two characteristics, *Starkus* n. gen. distinguishes itself from members of the 'plicatus' and 'trispinosus' groups, *Ty. aequiremis*, *Ty. finmarchicus*, and *Ty. kussakini*, all of which have one-articled exopod and endopod. Seven other typhlotanid species with parallel pereonite lateral margins (e.g., *Ty. assimilis*, *Ty. guca*, *Ty.*

*inaequipes*, *Ty. proctagon*, *Ty. profundus*, *Ty. plebejus*, and *Ty. williamsae* have one-articulated uropodal exopod and therefore could not be included in the new genus. Furthermore, *Starkus* n. gen. lacks the strong distal spines on pleotelson present in members of the ‘*spinicauda*’ group (*Typhlotanais spinicauda* Hansen, 1913, *Typhlotanais squamiger* Błażewicz-Paszkowycz, 2007a, *Typhlotanais priscilae* Segadilha & Serejo, 2022) and has pereopods 4–6 unguis simple (bifurcated in *Typhlotanais kyphosis*). Relatively robust cheliped (2.4 L:W) allows distinguishing *Starkus* n. gen. from *Typhlotanais longicephala*, with a much slender cheliped (4.0 L:W). Finally, *Baratheonus* n. gen. resembles *Starkus* n. gen. by the straight pereonite margins, slender chelipeds with basis separated by a gap from pereonite-1, relatively large prickly tubercles on the carpus of pereopods 4–6, and dorsodistal setae on pereopods 4–6 propodus. However, *Starkus* n. gen. has spines on pereopods 2–3 carpus and propodus, while *Baratheonus* n. gen. has setae, and biarticulated uropodal rami which are unarticulated in *Baratheonus* n. gen.

Parallel pereonites, biarticled uropods with exopod slightly longer than endopod, and antennule article-1 and cheliped covered with numerous ‘scales’ suggest that *Typhlotanais simplex* might belong to *Starkus* n. gen. Paratypes of this species are probably lost, but the holotype is kept at the Zoological Museum of Moscow (Mc1007). Unlike the other species currently classified to *Starkus* n. gen., *S. mimosis* has prominent spurs on pereopods 1–3 coxa (as found in *Antiplotanais*, the ‘*greenwichensis*’ group and *Typhlotanais compactus*) and gently rounded pereonites (straight in other *Starkus* n. gen.).

## *Starkus sirene* n. sp.

LSID urn:lsid:zoobank.org:act:982AB998-BA7D-41A9-940B-191555576A7B

(Figures 7–11)

### Material examined

Holotype, St. 9-12, neuter (2.0 mm, ZMHK-62843, illustrated). Paratypes. St. 12-4, neuter 1.4 mm (ZMHK-62844); St. 2-10, two neuters: 1.1 mm (ZMHK-62845), individual broken (ZMHK-62846); St. 7-9, two neuters: 1.3 mm (ZMHK-62847), 1.7 mm (ZMHK-62848); St. 7-10, neuter broken (ZMHK-62849); St. 10-9, two neuters: 1.5 mm (ZMHK-62850), individual broken (ZMHK-62851, dissected on slides), manca-3, 0.3 mm (ZMHK-62852); St. 11-9, five neuters, 0.8 mm (ZMHK-62853), 0.8 mm (ZMHK-62854), three individuals broken (ZMHK-62855; ZMHK-62856; ZMHK-62857); St. 12-4, 18 neuters: 0.5 mm (ZMHK-62858), 0.6 mm (ZMHK-62859); 0.9 mm (ZMHK-62860), 1.2 mm (ZMHK-62861); 1.3 mm (ZMHK-62862); 1.4 mm (ZMHK-

62863); 1.4 mm, (ZMHK-62864, dissected on slides); 1.43 mm (ZMHK-62865, dissected on slides); 1.6 mm (ZMHK-62866, in tube); 1.7 mm (ZMHK-62867); five individuals broken (ZMHK-62868; ZMHK-62869; ZMHK-62870; ZMHK-62871; ZMHK-62872); St. 9-12, neuter 1.5 mm (ZMHK-62873); St. 8-12, neuter 1.7 mm (ZMHK-62874); St. 9-12, three neuters: 1.4 mm, 1.7 mm, 1.8 mm (ZMHK-62875); St. 2-10, neuter 1.6 mm (ZMHK-62876); St. 2-10, neuter 1.1 mm (ZMHK-62877); St. 1-11, four neuters: 1.3 mm, 1.4 mm, 1.7 mm and 2.3 mm (ZMHK-62878); St. 10-9, neuter 2.3 mm (ZMHK-62879); St. 8-9, neuter 1.2 mm (ZMHK-62880); St. 2-9, two neuters: 1.1 mm and 1.2 mm (ZMHK-62881); St. 3-9, neuter 1.2 mm (ZMHK-62882); St. 3-9, five neuters: 1.5 mm, 1.7 mm, 1.8 mm, 2.2 mm, 2.5 mm and one dissected on slides (ZMHK-62883); St. 8-12, manca-3 1.7 mm (ZMHK-62884); St. 2-9, three neuters (ZMHK-62885, one broken and two in tube); St. 8-9, neuter 1.7 mm (ZMHK-62886); St. 9-9, three neuters: 1.6 mm, 1.8 mm, one broken (ZMHK-62887); St. 2-9, four neuters: 1.5 mm, 1.7 mm, 1.9 mm and 2.1 mm (ZMHK-62888). St. 2-10, adult (swimming) male 1.19 mm (broken, ZMHK-62890).

**Adult (swimming) male.** St. 2-9, 1.42 mm dissected on the slides (ZMHK-62890).

### Other material examined

St. 9-9, neuter broken (ICUL7938\*); St. 11-12, neuter broken (ICUL7943\*); St. 12-4, neuter 0.8 mm (ICUL7909\*).

\*Individual not recovered after DNA extraction.

### Diagnosis

Neuter: Body long (~7.0 L:W). Carapace 1.4 L:W. Pereonites straight in dorsal view. Antennule, antennae, and cheliped with ornamentation (‘scales’). Cheliped carpus 2.6 L:W, propodus 0.9× carpus. Cheliped basis length 0.8× cheliped carpus. Pereopods 1–3 coxa without spur; pereopod-2 merus with long seta; pereopods 2–3 propodus with strong seta; pereopods 4–6 merus ornamentation with two unequal spines. uropod exopod articles subequal.

Adult male (swimming). Pleon elongate, 0.4× TBL, with caudal process, pointed, without terminal spine. Antennule seven-articled, article-1 1.8 L:W; article-7 4.8 L:W, 0.7 article-6; cheliped carpus 2.7 L:W, chela 1.5× carpus; pereopod-4 dactylus and unguis together longer than propodus; pereopod-6 propodus with the row of scales along the article; uropod endopod two-articled, proximal article 0.9× distal article, exopod one-articled, 0.7× endopod proximal article.

### Etymology

From the Latin *siren* means a mythological being, her scaly tail, referring to ‘scales’ on the antennule, the antenna, and the cheliped.

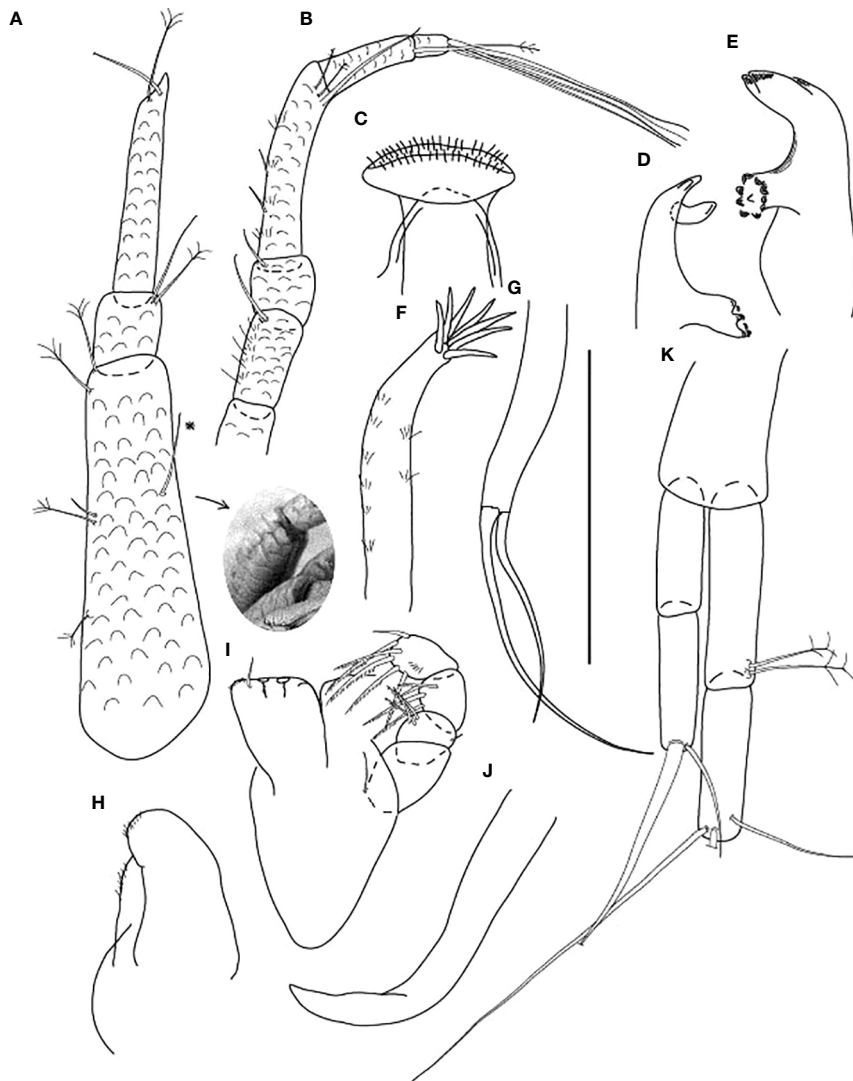


FIGURE 8

*Starkus sirene* n. sp., neuter: (A) Antennule (ZMHK-62883) and SEM image showing its 'scales' (ZMHK-62875); (B) Antenna (ZMHK-62864); (C) Labrum (ZMHK-62864); (D) Left mandible (ZMHK-62864); (E) Right mandible (ZMHK-62864); (F) Maxillule (ZMHK-62864); (G) Palp (ZMHK-62864); (H) Labium (ZMHK-62864); (I) Maxilliped (ZMHK-62864); (J) Epignath (ZMHK-62864); (K) Uropods (ZMHK-62864). Scale: (A–K) = 0.1 mm.

## Description

of neuter, length 1.5 mm. Body (Figures 7A, B) slender, 6.8 L:W. Cephalothorax with the short and pointy rostrum, 1.4 L:W, 3.1× pereonite-1, naked. Eyes absent. Pereonites margins straight and parallel, pereonites 1–6: 0.5, 0.8, 0.9, 0.9, 0.8, and 0.8 L:W, respectively; pereonite-1 trapezoidal, 0.7× pereonite-2; pereonite-2 trapezoidal, 0.9× pereonite-3; pereonites 3–4 square, all the same size; pereonite-5 square, 1.2× pereonite-6; pereonite-6 square. Pleon 0.2× TBL, with five subequal pleonites. Pleonites 1–5 the same size 0.3 L:W. Pleotelson 2.6× pereonite-6.

Antennule (Figure 8A) slightly shorter than cephalothorax, with 'scales'; article-1 0.6× antennule length, 4.0 L:W, with one chemosensory, three (two penicillate medial) setae, and two

penicillate distal setae; article-2 1.3 L:W, 0.2× article-1, with two (one penicillate distal) setae; article-3 7.1 L:W, 2.8× article-2, with terminal spur, one penicillate and one distal setae (other setae broken).

Antenna (Figure 8B) of six articles; all articles with 'scales'; article-1 broken; article-2 2.0 L:W, with long dorsodistal seta; article-3 1.1 L:W, 0.8× article-2, with dorsodistal seta; article-4 4.8 L:W, 3.0× article-3, with two fine medial setae and one long and two penicillate distal setae; article-5 3.6 L:W, 0.5× article-4, with long penicillate distal seta; article-6 minute, with four long distal setae.

Mouthparts. Labrum (Figure 8C) rounded, distal surface setose. Mandible Figures 8D, E) molar broad, edges with

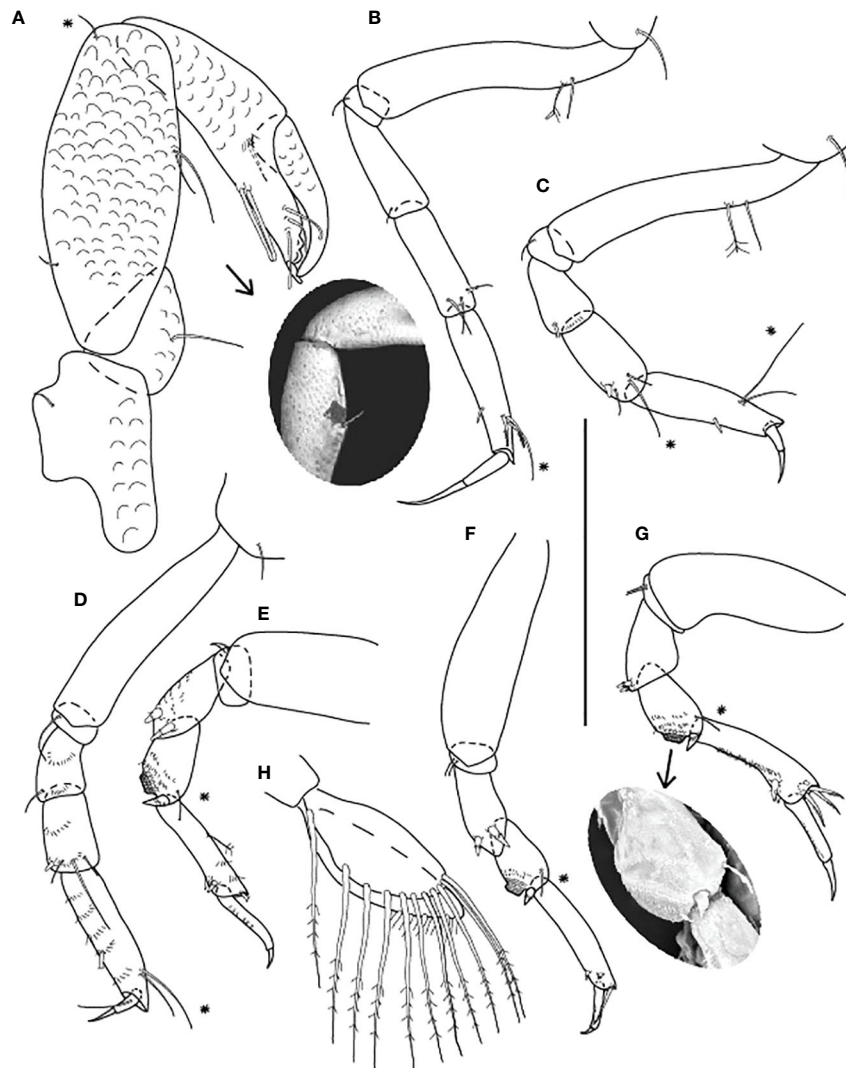


FIGURE 9

*Starkus sirene* n. sp., neuter: (A) Cheliped (ZMHK-62865) and SEM image showing 'scales' (ZMHK-62851); (B) Pereopod-1 (ZMHK-62883); (C) Pereopod-2 (ZMHK-62883); (D) Pereopod-3 (ZMHK-62883); (E) Pereopod-4 (ZMHK-62883); (F) Pereopod-5 (ZMHK-62851); (G) Pereopod-6 (ZMHK-62865) and SEM image showing prickly tubercles (clinging apparatus) (ZMHK-62851); (H) Pleopods. Scale: (A–H) = 0.1 mm.

prominent tubercles and spines; left mandible (Figure 8D) incisor (shape of one blunt tooth), *lacinia mobilis* well developed, with one lobe; right mandible (Figure 8E) incisor distal margin with two blunt teeth, without *lacinia mobilis*. Maxillule (Figure 8F) endite with at least seven terminal spines and scales on outer margin; palp (Figure 8G) with two distal setae. Labium (Figure 8H) distal margin finely setose; outer lobe membranous. Maxilliped (Figure 8I) basis 1.9 L:W; endites unfused, with two cusps and distal seta; palp with four articles; article-1 naked; article-2 wedge with three serrated inner setae and small outer seta; article-3 with four serrated inner setae; article-4 with six inner setae. Epignath (Figure 8J) curved, simple distally.

Cheliped (Figures 7C, 9A) separated by a gap from pereonite-1, with 'scales'; basis 1.7 L:W, with dorsal seta; merus subtriangular, with ventral seta; carpus 2.4 L:W, with two ventral setae, and one dorsoproximal and one dorsodistal chemosensory setae; chela 0.9× carpus, 3.6 L:W; palm as long as a fixed finger, with seta near dactylus insertion (on the inner surface); fixed finger with two long rod ventral setae; cutting edge with three rod setae and two weak, blunt cusps distally.

Pereopod-1 (Figure 9B) walking type, overall 18 L:W; coxa with seta; basis 6.0 L:W, with two (one penicillate dorsoproximal) setae; ischium with ventral seta; merus 2.9 L:W, with ventrodorsal seta; carpus 3.2 L:W, with three distal setae; propodus 4.9 L:W with one chemosensory and two serrated dorsodistal setae, and ventral



FIGURE 10  
*Starkus sirene* n. sp., swimming male (ZMHK-62890): (A) Antennule; (B) Antenna; (C) Maxilliped; (D) Labrum; (E) Uropods. Scale: (A–E) = 0.1 mm.

subdistal spine; dactylus  $0.7\times$  unguis, dactylus and unguis combined  $0.8\times$  propodus; unguis simple.

Pereopod-2 (Figure 9C) walking type, overall 15 L:W; coxa with seta; basis 6.7 L:W, with two (one penicillate dorsoproximal) setae; ischium with ventral seta; merus 1.8 L:W, with ventrodistal seta and distal numerous microtrichia; carpus 2.0 L:W,  $0.8\times$  merus, with one chemosensory and two short distal setae, and medial spine; propodus 4.1 L:W, with ventrodistal spine, one chemosensory and one dorsodistal setae; dactylus  $0.8\times$  unguis, both combined  $0.5\times$  propodus; unguis simple.

Pereopod-3 (Figure 9D) walking type, overall 14 L:W; coxa with seta; basis 5.3 L:W, naked; ischium with ventral seta; merus 1.7 L:W, with scales and ventrodistal seta; carpus 2.0 L:W,  $1.3\times$

merus, with scales on ventral margin, three distal setae and ventrodistal spine; propodus 4.3 L:W, with scales, one chemosensory and one dorsodistal setae and ventrodistal spine; dactylus  $0.9\times$  unguis, with proximal seta (longer than unguis); both combined  $0.3\times$  propodus; unguis simple.

Pereopod-4 (Figure 9E) clinging type; coxa and basis broken during dissection; ischium with ventral seta; merus 2.5 L:W, with scales and two unequal ventrodistal spines; carpus 2.0 L:W, with large, rounded area covered by minute spines (prickly tubercles) and dorsodistal chemosensory seta; propodus 5.7 L:W, with row of scales, one penicillate dorsal, one minute distal setae and two ventrodistal spines; dactylus  $5.3\times$  unguis, both combined  $0.8\times$  propodus; unguis simple.

Pereopod-5 (Figure 9F) as pereopod-4, but overall 8.4 L:W; coxa absent; basis 4.3 L:W, naked; propodus distal seta as long as dactylus.

Pereopod-6 (Figure 9G) as pereopod-4, but propodus with three dorsodistal setae reaching half of dactylus; dactylus and unguis about as long as propodus.

Pleopods (Figure 9H) basal article naked; exopod with six plumose setae on outer margin; endopod with ten plumose setae on outer margin; gap between proximal seta and the other setae.

Uropod (Figure 8K) both rami two-articled; exopod 0.8× endopod, proximal article 2.9 L:W, distal article 3.6 L:W with one strong and one setae; endopod proximal article 4.3 L:W, with two penicillate setae, distal article 3.5 L:W, with three long terminal setae (one broken).

**Description** of adult male, length 1.42 mm. Body (Figure 7D) slender, 5.3 L:W. Cephalothorax 1.1 L:W, 5.0× pereonite-1, naked. Eyes absent. Pereonites 1–6 oval-shaped: 0.2, 0.3, 0.3, 0.3, 0.4, and 0.4 L:W, respectively. Pereonite-1 0.7× pereonite-2; pereonite-2 0.9× pereonite-3; pereonite-3 1.2× pereonite-4; pereonite-4 0.8× pereonite-5; pereonite-5 as long as pereonite-6. Pleon elongate, 0.4× BL, with five subequal pleonites. Pleonites 1–5: 0.3, 0.3, 0.3, 0.3, and 0.5 L:W. Pleotelson pointed 5.4× pereonite-6.

Antennule (Figure 10A) 1.6× cephalothorax, seven-articled, article-1 0.3× antennule length, 1.8 L:W, with three penicillate and two ventrodiscal setae; article-2 0.9 L:W; 0.5× article-1, with three distal setae; article-3 1.0 L:W; 0.6× article-2, with two dorsodistal setae; article-4 0.8 L:W, 0.4× article-3, with numerous aesthetascs distally; article-5 1.2 L:W, 1.3× article-4, with numerous aesthetascs distally; article-6 3.9 L:W, 2.3× article-5, with numerous aesthetascs distally; article-7 4.8 L:W, 0.7× article-6, with long and four short setae distally.

Antenna (Figure 10B) of seven articles; article-1 lost during dissection; article-2 1.5 L:W, with long dorsodistal seta; article-3 1.5 L:W, 0.8× article-2, with long dorsodistal seta; article-4 2.6 L:W; 1.2× article-3, with penicillate distal seta; article-5 5.5 L:W, 1.8× article-3, with two penicillate medial, one penicillate and three distal (two long and one short) setae; article-6 7.0 L:W, as long as article-4, with two long distal setae; article-7, 1.5 L:W with three long distal setae.

Mouthparts. Labrum (Figure 10C) simple, rounded, naked corners. Mandible, maxillule, and maxilla not recovered during dissection. Maxilliped (Figure 10D) basis fused. Endites reduced, simple, and rounded; palp article-1 naked, article-2 with two inner setae; article-3 with two long and one short inner setae; article-4 relatively slender, with five long distal setae.

Cheliped (Figure 11A) basis 1.2 L:W, distally rounded, attached to carapace by semi-oval sclerite; merus wedge, with ventral seta (broken); carpus twice as long as wide, with two midventral setae, one short and one chemosensory setae on dorsal margin; chela 1.3× carpus, 2.7 L:W; palm 1.5 L:W with row of 15 spines on the inner surface near dactylus insertion; dactylus with sharp terminal spine and with two minute spines

on cutting edge; fixed finger cutting edge serrated, with three setae; distal spine robust, pointed 4.0 L:W.

Pereopod-1 (Figure 11B) walking type; basis 6.0 L:W, naked; ischium with ventral seta; merus 3.2 L:W, with ventrodiscal seta; carpus 5.0 L:W, 1.3× merus, with one dorsodistal and one ventrodiscal (broken) setae; propodus 9.0 L:W, with ventrodiscal seta; dactylus and unguis broken.

Pereopod-2 (Figure 11C) walking type; basis 5.8 L:W, naked; ischium with ventral seta; merus 2.7 L:W, with two short ventrodiscal setae; carpus 3.8 L:W, 1.3× merus, with long dorsodistal and two ventrodiscal setae; propodus 6.3 L:W, with short, dorsodistal and short ventrodiscal setae; dactylus and unguis broken.

Pereopod-3 (Figure 11D) similar to pereopod-2, but carpus and propodus with numerous scales.

Pereopod-4 (Figure 11E) overall 17 L:W; coxa absent; basis 7.3 L:W, naked; ischium with two ventral setae (long and short); merus 3.4 L:W, with two ventral setae; carpus 3.3 L:W, three distal setae; propodus 6.3 L:W, with three (one dorsodistal and two ventrodiscal) setae with numerous scales; dactylus 1.5× unguis, both combined 1.5× propodus.

Pereopod-5 (Figure 11F) coxa absent; basis 5.2 L:W, with three (one penicillate dorsoproximal and one penicillate ventral) setae; ischium with two ventral setae (long and short); merus 3.3 L:W, with two ventrodiscal setae; carpus 4.6 L:W, with three distal setae; propodus 7.0 L:W, with numerous scales; dactylus and unguis broken.

Pereopod-6 (Figure 11G) as pereopod-5, but basis naked.

Pleopods (Figure 11H) basal article naked; exopod with seven plumose setae on outer margin and one on inner margin; endopod with seven plumose setae on outer margin.

Uropod (Figure 10E) basal article as long as wide; exopod one-articled, 0.3× endopod length, with medial seta, one robust and one small distal setae; endopod proximal article 3.2 L:W, with six penicillate medial and two penicillate distal setae; distal article as long as proximal, with medial seta (broken), tipped by two setae (broken) and two setae distally.

## Distribution

*Starkus sirene* n. sp. is known from nine locations off the Kuril-Kamchatka Trench in a depth range of 4859–5643 m (Figure 1).

## Remarks

The adult male *Starkus sirene* n. sp. has a swimming habitus that is morphologically so different from the female that without the use of molecular methods, species identification of these males would not be possible.

The distribution of three scales allow to distinguish the *Starkus* species. In *Starkus sirene* n. sp., the scales cover the antennules, antennae, and cheliped, whereas in *S. mixtus* those structures are present only at article 1 (Appendix 2). Both taxa can be distinguished by the setation of pereopod-2 merus (one seta in *Starkus sirene* n. sp. and two setae in *S. mixtus*). Finally, uropod exopod articles are subequal in *Starkus sirene* n. sp., but article-1 is longer than article-2

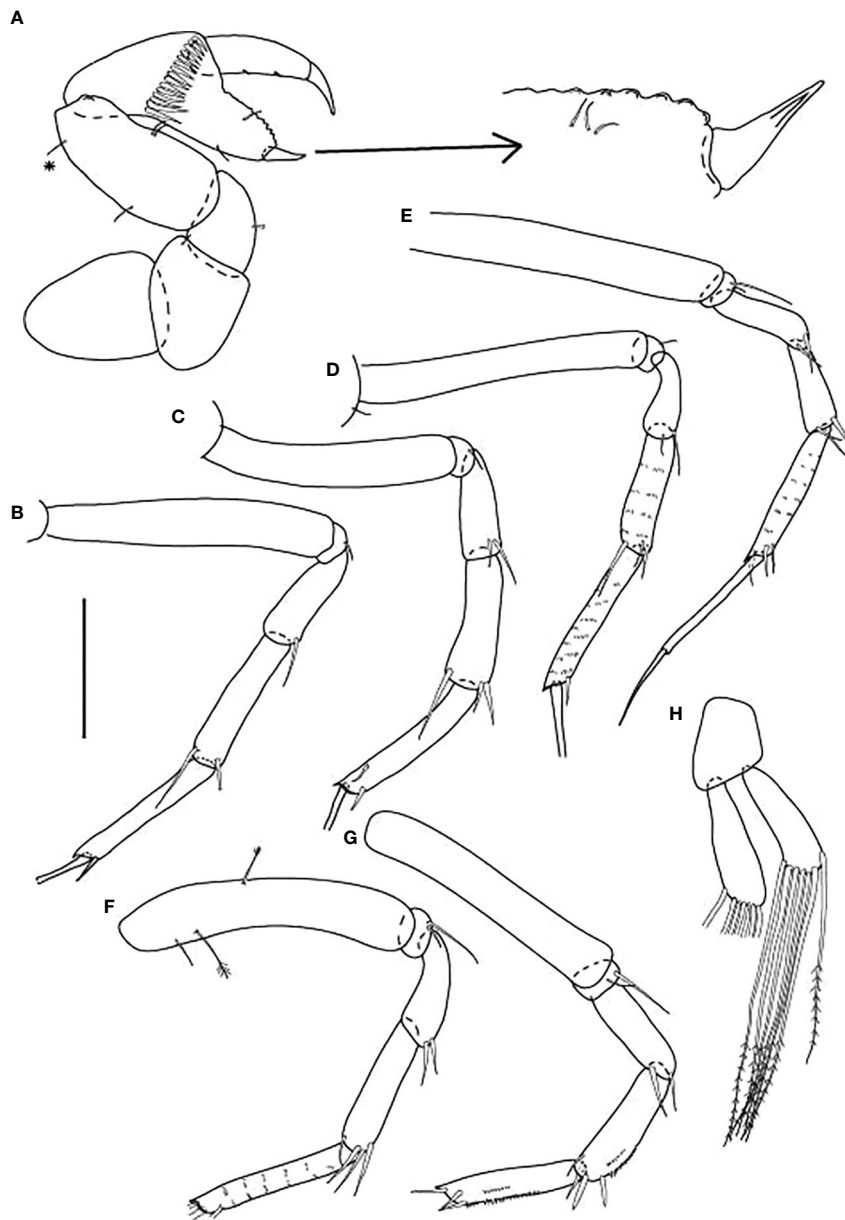


**FIGURE 11**  
*Starkus sirene* n. sp., swimming male (ZMHK-62890): (A) Cheliped; (B) Pereopod-1; (C) Pereopod-2; (D) Pereopod-3; (E) Pereopod-4; (F) Pereopod-5; (G) Pereopod-6; (H) Pleopods. Scale: (A–H) = 0.1 mm.

in *S. mixtus*. Apart from the characteristic scales of *Starkus. sirene* n. sp., which are absent in *S. mimosis* and *S. simplex*, *Starkus sirene* n. sp. has pereopod-2 merus with distal seta, *S. mimosis* has two short setae, and *S. simplex* has three distal setae there.

**Key for identification of *Starkus* females**

- 1. Pereopods 1–3 coxa with spur.....  
 .....*S. mimosis* (Błażewicz-Paszkowycz, 2007a)

- (W Antarctic, 2659–4655 m)  
 -Without spur .....2
- 2. Cheliped basis length 0.8× cheliped carpus.....  
 .....*Starkus sirene* n. sp.  
 (Kuril-Kamchatka, 4859–5643 m)
- Cheliped basis length 0.6× cheliped carpus .....3
- 3. Antennule article-1 ornamentation: two groups of simple setae and pinnate medial setae and distally and ‘scales’

- .....*S. mixtus* (Hansen, 1913)  
(N Atlantic, 906–2626 m)
- Antennule article-1 ornamentation: inner penicillate seta at mid-length and simple and pinnate setae distally distally
- .....*S. simplex* (Kudinova-Pasternak, 1984)  
(N Pacific, 455–1356 m)

**DNA analyses**

A total of six different COI haplotypes and nine 18S haplotypes were newly obtained from the University of Lodz Tanaidacea collection (GenBank accession numbers: ON310832–ON310845 for COI and ON255540–ON255555 for 18S rDNA; see Table 3). The COI sequence alignment included a total of 615 bp, and the BIC method selected the Hasegawa–Kishino–Yano (HKY) DNA substitution model with a gamma parameter ( $G = 0.86$ ) and with a proportion of invariant sites ( $I = 0.22$ ). The 18S rDNA alignment included 1,033 bp, and the BIC method selected the Kimura 2 parameter (K2P) DNA substitution model with gamma parameter ( $G = 0.36$ ) and with a proportion of invariant sites ( $I = 0.42$ ). Single gene trees were congruent, and the Maximum Likelihood tree with the highest log-likelihood ( $L_n = -5183.89$ ) obtained after both alignments were concatenated is shown in Figure 12. Several well-supported monophyletic clades were recovered, such as the so-called ‘short-bodied’ forms (i.e., *Typhlotanais cornutus* G.O. Sars, 1879, grouping with *Typhlotanais eximius* Hansen, 1913) and a clade including representatives of the ‘collar’ forms (e.g., *Typhlotanais variabilis* Hansen, 1913, and *Torquella cf. grandis*). Consequently, our preliminary molecular phylogeny suggests the polyphyly of the genus *Typhlotanais*, with ‘collar’ species forming a monophyletic clade together with *Torquella*. *Typhlamia* and

*Pulcherella* formed a well-supported monophyletic clade, while *Starkus sirene* n. sp. and *S. mixtus* clustered with a putative *Typhlotanais finmarchicus* sequence obtained from GenBank (MN337129.1). The clade grouping all ‘long-bodied’ forms of Typhlotanidaea (except *Baratheonus* n. gen.) presents marginal bootstrap support (70%), and it is characterized by including species with a third seta on the cheliped carpus ventral margin.

The typhlotanid lineages analyzed seem to have evolved independently long ago, and pairwise COI genetic distances between groups ranged up to 0.552 (Table 4). The largest genetic divergences were observed when comparing *Pulcherella pulcher* (Hansen, 1913) with *Starkus sirene* n. sp. ( $p\text{-dist} = 0.341 \pm 0.021$ ;  $K2P = 0.463 \pm 0.039$ ) or *Ty. variabilis* ( $p\text{-dist} = 0.340 \pm 0.018$ ;  $K2P = 0.458 \pm 0.037$ ). For comparison, smallest genetic distances were found between *Torquella cf. grandis* and *Ty. variabilis* ( $p\text{-dist} = 0.270 \pm 0.018$ ;  $K2P = 0.339 \pm 0.027$ ) or *Ty. cornutus* and *Ty. eximius* ( $p\text{-dist} = 0.277 \pm 0.020$ ;  $K2P = 0.355 \pm 0.033$ ). As with the Maximum Likelihood tree, genetic distances suggest that *Typhlotanais* is not monophyletic, and several species currently classified to this genus may represent distinct genera.

**Environmental correlation analyses**

Abundance and diversity of the Typhlotanidaea collection were largest at the southernmost station (i.e., St. 12-4; see Table 2 and Figure 1). Four other stations (St. 9-9, 9-12, 10-9, and 10-12), which cluster together in an abyssal plain area surrounded by a seamount ridge, included 67.5% of all *Typhlamia genesis* n. sp. individuals. The Cumulative Relative Frequency and the factor analysis show that the relative number of *Typhlamia genesis* n. sp. individuals increased with depths below 5,200 m, as opposed to *Baratheonus roberti* n. sp. and *Starkus sirene* n. sp. which apparently prefer

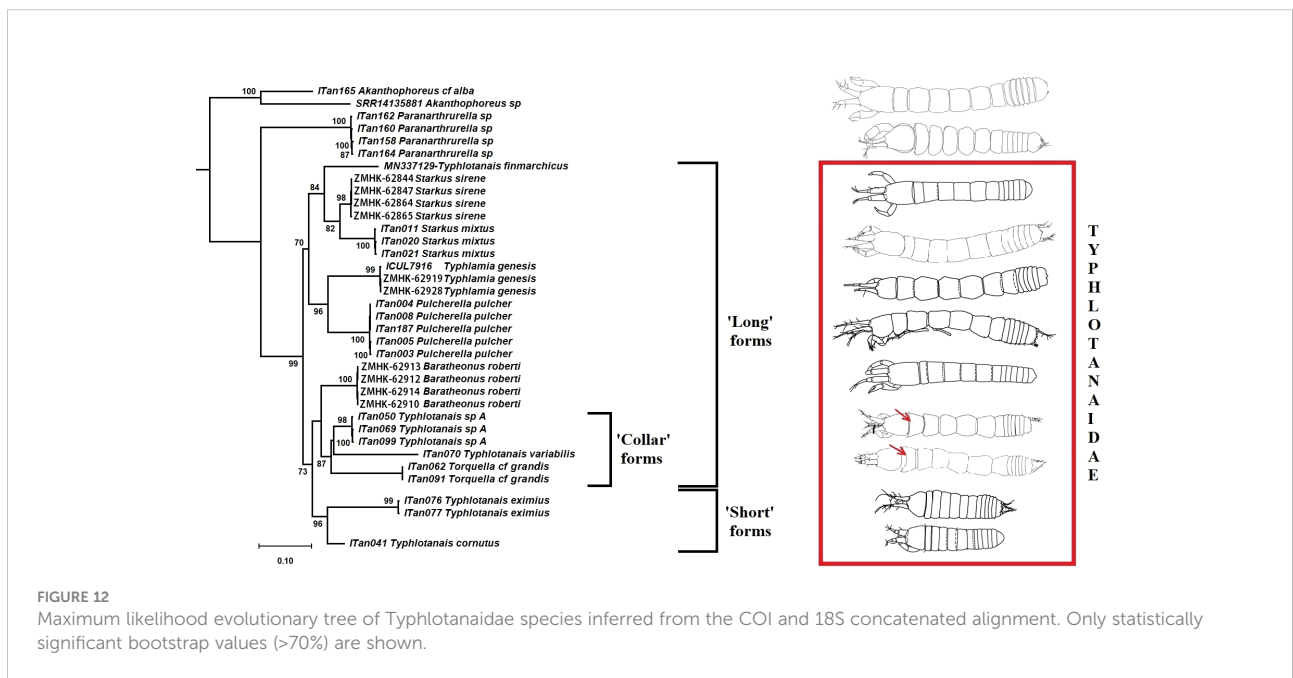


FIGURE 12 Maximum likelihood evolutionary tree of Typhlotanidaea species inferred from the COI and 18S concatenated alignment. Only statistically significant bootstrap values (>70%) are shown.

TABLE 3 Voucher codes for the museum specimens and GenBank accession numbers for the COI and 18S rDNA sequences used to build the molecular tree.

Species	Voucher	COI (GenBank accession numbers)	18S rDNA (GenBank accession numbers)	Reference
<i>Akanthophoreus cf. alba</i>	ITan165		ON255554	Present study
<i>Akanthophoreus</i> sp.	–	SRR14135881	ON255555	SRA database; present study
<i>Paranarthrurella</i> sp.	ITan158	MK751352	MK804177	Błażewicz et al. (2019)
<i>Paranarthrurella</i> sp.	ITan160	MK751354	MK804178	Błażewicz et al. (2019)
<i>Paranarthrurella</i> sp.	ITan162		MK804179	Błażewicz et al. (2019)
<i>Paranarthrurella</i> sp.	ITan164	MK751357		Błażewicz et al. (2019)
<i>Baratheonus roberti</i> n. sp.	ZMHK-62910	ON310832		Present study
<i>Baratheonus roberti</i> n. sp.	ZMHK-62914	ON310837		Present study
<i>Baratheonus roberti</i> n. sp.	ZMHK-62912	ON310838	ON255543	Present study
<i>Baratheonus roberti</i> n. sp.	ZMHK-62913	ON310841	ON255545	Present study
<i>Pulcherella pulcher</i>	ITan003	KJ934617	ON255546	Błażewicz-Paszkowycz et al. (2014); present study
<i>Pulcherella pulcher</i>	ITan004	KJ934618		Błażewicz-Paszkowycz et al. (2014)
<i>Pulcherella pulcher</i>	ITan005	KJ934619	ON255547	Błażewicz-Paszkowycz et al. (2014); present study
<i>Pulcherella pulcher</i>	ITan008	KJ934620		Błażewicz-Paszkowycz et al. (2014)
<i>Pulcherella pulcher</i>	ITan187	KJ934621		Błażewicz-Paszkowycz et al. (2014)
<i>Starkus sirene</i> n. sp.	ZMHK-62865	ON310833	ON255540	Present study
<i>Starkus sirene</i> n. sp.	ZMHK-62864	ON310834	ON255541	Present study
<i>Starkus sirene</i> n. sp.	ZMHK-62844	ON310835		Present study
<i>Starkus sirene</i> n. sp.	ZMHK-62847	ON310839	ON255544	Present study
<i>Torquella cf. grandis</i>	ITan062	KJ934614		Błażewicz-Paszkowycz et al. (2014)
<i>Torquella cf. grandis</i>	ITan091	KJ934613		Błażewicz-Paszkowycz et al. (2014)
<i>Typhlamia genesis</i> n. sp.	ICUL7916	ON310836	ON255542	Present study
<i>Typhlamia genesis</i> n. sp.	ZMHK-62928	ON310840		Present study
<i>Typhlamia genesis</i> n. sp.	ZMHK-62919	ON310842		Present study
<i>Typhlotanais cornutus</i>	ITan041	MK751360	ON255551	Błażewicz et al. (2019); present study
<i>Typhlotanais eximius</i>	ITan076	MK751361		Błażewicz et al. (2019)
<i>Typhlotanais finmarchicus</i>	WS 12845		MN337129	GenBank database
<i>Typhlotanais mixtus</i>	ITan011	ON310843	ON255548	Present study
<i>Typhlotanais mixtus</i>	ITan020		ON255549	Present study
<i>Typhlotanais mixtus</i>	ITan021	ON310844	ON255550	Present study
<i>Typhlotanais</i> sp. A	ITan050	KJ934599		Błażewicz-Paszkowycz et al. (2014)
<i>Typhlotanais</i> sp. A	ITan069	KJ934600	ON255552	Błażewicz-Paszkowycz et al. (2014); present study
<i>Typhlotanais</i> sp. A	ITan099	KJ934601	ON255553	Błażewicz-Paszkowycz et al. (2014); present study
<i>Typhlotanais variabilis</i>	ITan070	KJ934605		Błażewicz-Paszkowycz et al. (2014)
<i>Typhlotanais variabilis</i>	ITan077	ON310845		Present study

The body of voucher ICUL7916 could not be recovered after DNA extraction.

shallower waters (>60% of the specimens recovered for those two species were found above 5,200-m depth; Figure 13). Although *Baratheonus roberti* n. sp. and *Starkus sirene* n. sp. have a similar depth distribution, environmental requirements among them seem to differ. While *Baratheonus roberti* n. sp. was found in areas with larger variation in dissolved oxygen and comparatively strong bottom currents, *Starkus sirene* n. sp. appears usually at stations with lower oxygen concentration and slower bottom currents (Table 2). Non-parametric correlation shows that *Typhlamia genesis* n. sp. abundance is lowest in stations with

higher amounts of silica (−0.546), calcium (−0.583), and strontium (−0.568), whereas it is most abundant in areas rich in manganese (0.602) and potassium (0.606) (Appendix 3). *Starkus sirene* n. sp. is abundant in places rich in organic carbon (0.456), and *Baratheonus roberti* n. sp. shows no significant correlation (positive or negative) with the environmental variables recorded. The taxa studied here seem to have distinct ecological requirements, but data on environmental factors and species abundances are still lacking and more research is needed to confirm the results obtained here.

TABLE 4 Genetic distances among Typhlotanidae COI sequences.

	<i>Baratheonus roberti</i> n. sp.	<i>Paranarthrurella</i>	<i>Pulcherella pulcher</i>	<i>Starkus sirene</i> n. sp.	<i>Torquella cf. grandis</i>	<i>Typhlamia genesis</i> n. sp.	<i>Typhlotanais cornutus</i>	<i>Typhlotanais eximius</i>	<i>Typhlotanais variabilis</i>
<i>Baratheonus roberti</i> n. sp.		0.479 ± 0.041	0.404 ± 0.036	0.441 ± 0.038	0.343 ± 0.033	0.397 ± 0.034	0.404 ± 0.038	0.387 ± 0.038	0.401 ± 0.033
<i>Paranarthrurella</i>	0.350 ± 0.021		0.512 ± 0.040	0.497 ± 0.043	0.499 ± 0.044	0.532 ± 0.047	0.463 ± 0.042	0.532 ± 0.046	0.496 ± 0.040
<i>Pulcherella pulcher</i>	0.309 ± 0.020	0.368 ± 0.021		0.463 ± 0.039	0.438 ± 0.040	0.440 ± 0.040	0.445 ± 0.041	0.458 ± 0.040	0.458 ± 0.037
<i>Starkus sirene</i> n. sp.	0.330 ± 0.020	0.355 ± 0.020	0.341 ± 0.021		0.409 ± 0.036	0.420 ± 0.036	0.433 ± 0.038	0.396 ± 0.036	0.403 ± 0.034
<i>Torquella cf. grandis</i>	0.274 ± 0.019	0.357 ± 0.021	0.328 ± 0.019	0.311 ± 0.019		0.381 ± 0.033	0.392 ± 0.036	0.373 ± 0.035	0.339 ± 0.027
<i>Typhlamia genesis</i> n. sp.	0.304 ± 0.019	0.376 ± 0.020	0.326 ± 0.021	0.318 ± 0.020	0.298 ± 0.020		0.373 ± 0.034	0.386 ± 0.035	0.370 ± 0.031
<i>Typhlotanais cornutus</i>	0.308 ± 0.020	0.340 ± 0.020	0.333 ± 0.020	0.326 ± 0.021	0.301 ± 0.020	0.293 ± 0.019		0.355 ± 0.033	0.370 ± 0.031
<i>Typhlotanais eximius</i>	0.299 ± 0.020	0.371 ± 0.021	0.339 ± 0.021	0.303 ± 0.019	0.292 ± 0.020	0.301 ± 0.020	0.277 ± 0.020		0.354 ± 0.030
<i>Typhlotanais variabilis</i>	0.304 ± 0.019	0.354 ± 0.019	0.340 ± 0.018	0.308 ± 0.018	0.270 ± 0.018	0.290 ± 0.017	0.288 ± 0.019	0.279 ± 0.018	

P-distances (± SE) are shown below the diagonal, while Kimura-2P values are shown above the diagonal.

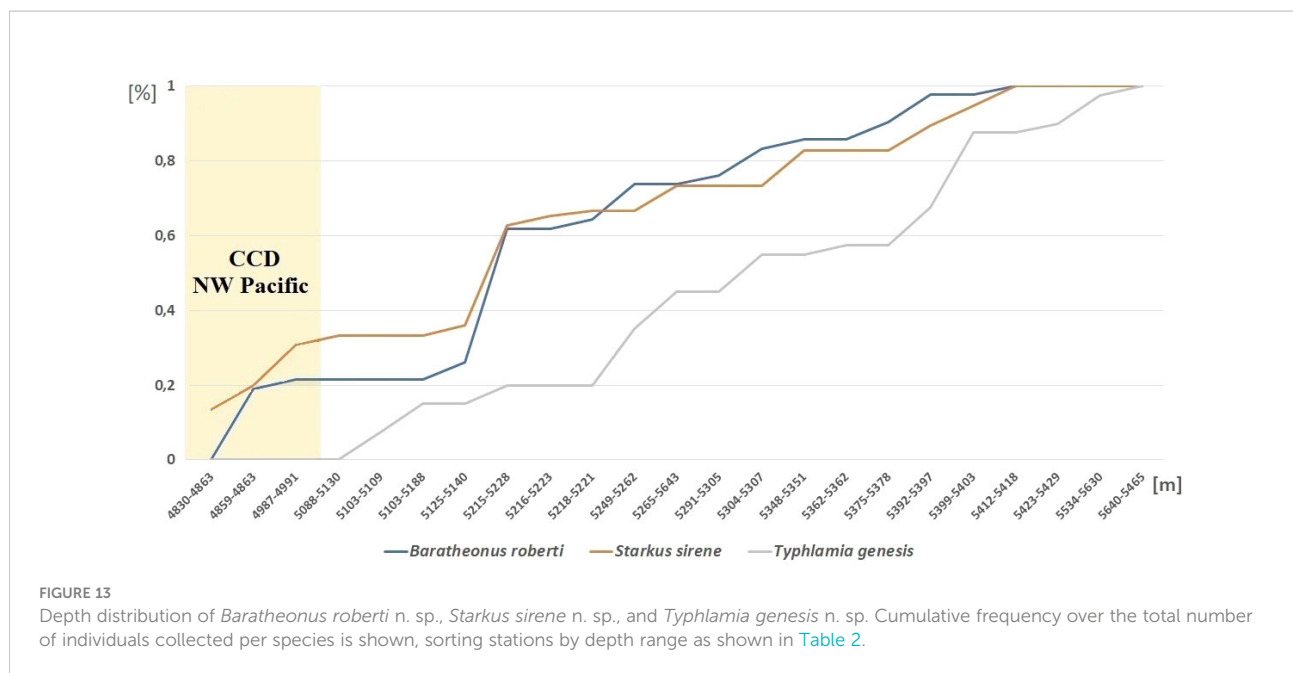
## Discussion

The first molecular phylogeny of Typhlotanidae is presented including descriptions of three new species and genera. The genetic clusters obtained, despite that one mitochondrial gene and one nuclear genes should be considered as preliminary results. It is congruent with morphological data (e.g., ‘short-bodied’ forms such as *Typhlotanais cornutus* and *Typhlotanais eximius* grouping together) and confirm the non-monophyly of *Typhlotanais*, as previously suggested by Błażewicz-Paszkowycz (2007a). Molecular results also support the monophyly of the so-called ‘collar’ form species, grouping taxa with a unique pereonite-1 shape. An integrative taxonomy approach, combining molecular and morphological evidence, allowed us to erect the new genus *Baratheonus* for a ‘long-bodied’ form with a particularly large and unique clinging apparatus and *Starkus* n. gen. for the former ‘mixtus’ morpho-group (Błażewicz-Paszkowycz, 2007a). A detailed morphological analysis has revealed the heterogeneity of the so-called clinging apparatus of typhlotanids, a complex system of hooks, tubercles, thorns, and spines, located on the carpi of pereopods 4–6 (see also Błażewicz-Paszkowycz, 2007a). Future evolutionary studies should include high-resolution images in a wider range of typhlotanid genera.

The use of molecular data allowed us to identify the male of *Starkus sirene* n. sp., confirming the strong sexual dimorphism of Paratanaoidea (Sieg, 1986; Błażewicz-Paszkowycz et al., 2014) and providing further details on typhlotanid male morphology.

Significant differences on the development and structure of antennules and chelipeds among males and females of *Starkus* n. gen. are also found in other typhlotanid genera for which males have been identified so far using genetic data (*Pulcherella*, *Torquella*, and *Typhlotanais*) (Błażewicz-Paszkowycz et al., 2014). Interestingly, male morphology is also congruent with the new preliminary phylogeny, with males of the so-called ‘collar’ forms (i.e., *Torquella cf. grandis* and *Typhlotanais* sp. A) showing similar, slightly pointed, pleotelson where other long-bodied genera (e.g., *Pulcherella* and *Starkus* n. gen.) present a strong projection (Błażewicz-Paszkowycz et al., 2014). The fact that *Starkus sirene* n. sp. females occurred throughout the study area while male specimens were only found at the northernmost stations might suggest that typhlotanid sex ratios vary across the species distribution. Although recent studies point toward ecological differences between sexes as the main cause behind sex ratio bias in crustaceans (Ewers-Saucedo, 2019), further geographic and taxonomical samplings are needed before claiming this is also the case for deep-sea Typhlotanidae.

Despite extensive sampling at the Sea of Japan (Kudinova-Pasternak, 1984; Błażewicz-Paszkowycz et al., 2013), Okhotsk Sea (Stępień et al., 2019), and the Kuril-Kamchatka Trench (Kudinova-Pasternak, 1966, 1970; Bamber, 2007; Bird, 2007; Błażewicz-Paszkowycz, 2007b; Larsen and Shimomura, 2007; McLelland, 2007), NW Pacific deep-sea Typhlotanidae were represented by just 15 species belonging to seven genera up to date. The KuramBio collection expands our current knowledge on the diversity and distribution of typhlotanids present in the NW



Pacific, significantly increasing the number of deep-sea species (by 42%) and genera (by 40%). Typhlotanidae occur in a wide bathymetric range, but most of them are found well beyond the Carbonate Compensation Depth (CCD), about 4,500 m in the Pacific (Morse and Mackenzie, 1990; Pälke et al., 2012). Despite that sediments below CCD are putatively free of calcium carbonate (Archer, 1996), many factors could be at play during biocalcification (Clark, 2020) and large and well-calcified tanaid genera *Gigantapseudes* Kudinova-Pasternak, 1978 and *Neotanais* Beddard, 1886, have been reported from the deepest oceanic trenches (Wolff, 1956; Messing, 1976; Gamo, 1984). More research is needed to better understand the mechanisms used by crustaceans to compensate the lack of calcium carbonate, and typhlotanids are ideal candidates that seem to be particularly adapted to cope with the extreme conditions of abyssal and deeper (hadal) zones. The preliminary phylogeny and new morphological evidence presented here will facilitate future studies through a better understanding of the diversity of deep-sea typhlotanids.

## Data availability statement

The datasets presented in this study can be found in online repositories. The names of the repository/repositories and accession number(s) can be found in the article/Supplementary Material.

## Author contributions

MB planned the research and obtained funding for the project. MG and MB studied and described the morphology of

the KuramBio typhlotanid specimens, and carried out molecular laboratory work. FP completed the phylogenetic analyses. All authors contributed to the article and approved the submitted version.

## Funding

The authors are most thankful to three anonymous reviewers, which significantly improved the manuscript. This study was funded by the Polish National Science grants UMO-2016/13/B/NZ8/02495 and 2021/41/N/NZ8/02039 and Grant Competition of The University of Lodz 4/DGB/IDUB/2022. FP acknowledges the project “CIDEAGENT/2019/028 - Biodiversity PATterns of Crustacea from Karstic Systems (BIOPACKS): molecular, morphological, and functional adaptations” funded by the Conselleria d’Innovació, Universitats, Ciència i Societat Digital.

## Acknowledgments

Many thanks are given to Maciej Studzian (University of Lodz) for help with carrying out the confocal microscopy imaging. We would also like to thank Agnieszka Rewicz (University of Lodz) for her help in showing and teaching the use of the scanning electron microscope. Thanks are due to the reviewers for significantly improving this manuscript through their comments.

## Conflict of interest

The authors declare that the research was conducted in the absence of any commercial or financial relationships that could be construed as a potential conflict of interest.

## Publisher's note

All claims expressed in this article are solely those of the authors and do not necessarily represent those of their affiliated

organizations, or those of the publisher, the editors and the reviewers. Any product that may be evaluated in this article, or claim that may be made by its manufacturer, is not guaranteed or endorsed by the publisher.

## Supplementary material

The Supplementary Material for this article can be found online at: <https://www.frontiersin.org/articles/10.3389/fmars.2022.927181/full#supplementary-material>

## References

- Altschul, S. F., Gish, W., Miller, W., Myers, E., and Lipman, D. J. (1990). Basic local alignment search tool. *J. Mol. Biol.* 215, 403–410. doi: 10.1016/S0022-2836(05)80360-2
- Archer, D. E. (1996). An atlas of the distribution of calcium carbonate in sediments of the deep sea. *Glob. Biochem. Cycles.* 10, 159–174. doi: 10.1029/95GB03016
- Bamber, R. N. (2007). Suborders Apeudomorpha Sieg, 1980 and Neotanaidomorpha Sieg, 1980. *Zootaxa* 1599, 13–40. doi: 10.11646/zootaxa.1599.1.3
- Bamber, R. N. (2008). Tanaidaceans (Crustacea: Peracarida: Tanaidacea) from Moreton Bay, Queensland. *Memoirs of the Queensland Museum* 1599, 13–40. doi: 10.11646/zootaxa.1599.1.3
- Beddard, M. A. (1886). Report on the Isopoda collected by H.M.S. *Challenger* during the years 1873–1876. Second Part. Report on the Scientific Results of the voyage of H.M.S. *Challenger* during the Years 1873–76. *Zoology* 17, 109–159. doi: 10.5962/bhl.title.6513
- Bird, G. J. (2004). The Tanaidacea (Crustacea, Peracarida) of the North-east Atlantic: The shelf and bathyal *Paratyphlotanais* of the 'Atlantic margin'. *J. Nat. Hist.* 54 (1), 143–1359.
- Bird, G. J. (2007). Families Anarthruridae Lang, 1971, Colletteidae Larsen & Wilson, 2002, and Leptognathiidae Sieg, 1976. Eds. K. Larsen and M. Shimomura Tanaidacea (Crustacea: Peracarida) From Japan III. The Deep Trenches: The Kurile-Kamchatka Trench and Japan Trench. *Zootaxa* 1599, 61–85. doi: 10.11646/zootaxa.1599.1.5
- Bird, G. J., and Larsen, K. (2009). Tanaidacean phylogeny – the second step: the basal paratanaoidean families (Crustacea: Malacostraca). *Arthropod. Syst. Phylogeny.* 67, 137–158.
- Błażewicz, M., Józwiak, P., Jennings, R.M., Studzian, M., and Frutos, I. (2019). Integrative systematics and ecology of a new deep-sea family of tanaidacean crustaceans. *Scientific Reports* 9, 1–70. doi: 10.1038/s41598-019-53446-1
- Błażewicz-Paszkowycz, M. (2007a). A revision of the family *Typhlotanaiidae* Sieg, 1984 (Crustacea: Tanaidacea) with the remarks on the *Nototanaiidae* Sieg, 1976. *Zootaxa* 1598, 1–141. doi: 10.11646/zootaxa.1598.1.1
- Błażewicz-Paszkowycz, M. (2007b). Family *Nototanaiidae* Sieg, 1976. and *Typhlotanaiidae* Sieg, 1984. Eds. K. Larsen and M. Shimomura. Tanaidacea (Crustacea: Peracarida) From Japan III. The Deep Trenches: The Kurile-Kamchatka Trench and Japan Trench. *Zootaxa* 1599, 101–120. doi: 10.5281/zenodo.178686
- Błażewicz-Paszkowycz, M., Bamber, R.N., and Anderson, G. (2012). Diversity of Tanaidacea (Crustacea: Peracarida) in the world's Oceans – How far have we come? *PLoS One* 7, 1–11. doi: 10.1371/journal.pone.0033068
- Błażewicz-Paszkowycz, M., Bamber, R.N., and Cunha, M.R. (2011). New tanaidomorph Tanaidacea (Crustacea: Peracarida) from submarine mud-volcanoes in the Gulf of Cadiz (North-east Atlantic). *Zootaxa* 2769, 1–53.
- Błażewicz-Paszkowycz, M., Bamber, R.N., and Józwiak, P. (2013). Tanaidaceans (Crustacea: Peracarida) from the SoJaBio joint expedition in slope and deeper waters in the Sea of Japan. *Deep. Res. Part II. Top. Stud. Oceanogr.* 86–87, 181–213. doi: 10.1016/j.dsr2.2012.08.006
- Błażewicz-Paszkowycz, M., Jennings, R. M., Jeskulle, K., and Brix, S. (2014). Discovery of swimming males of Paratanaoidea (Tanaidacea). *Polish. Polar. Res.* 35, 415–453. doi: 10.2478/popore-2014-0022
- Bober, J., Brandt, A., Frutos, I., and Schwentner, M. (2019). Diversity and distribution of Ischnomesidae (Crustacea: Isopoda: Asellota) along the Kuril-Kamchatka Trench – A genetic perspective. *Prog. Oceanogr.* 178, 1–12. doi: 10.1016/j.pocean.2019.102174
- Brandt, A., Elsner, N. O., Malyutina, M. V., Brenke, N., Golovan, O. A., Lavrenteva, A. V., et al. (2015). Abyssal macrofauna of the Kuril-Kamchatka Trench area (Northwest Pacific) collected by means of a camera-epibenthic sledge. *Deep. Res. Part II. Top. Stud. Oceanogr.* 111, 175–187. doi: 10.1016/j.dsr2.2014.11.002
- Brandt, A., Elsner, N. O., Malyutina, M. V., and Golovan, O. A. (2010). *The Russian-German deep-sea expedition (SoJaBio) to the Sea of Japan on board of the R/V Akademik Lavrentyev.* 1–52. doi: 10.13140/RG.2.1.1818.2809
- Brandt, A., and Malyutina, M. V. (2015). The German-Russian deep-sea expedition KuramBio (Kurile Kamchatka Biodiversity Studies) on board of the RV *Sonne* in 2012 following the footsteps of the legendary expeditions with RV *Vityaz.* *Deep. Res. Part II. Top. Stud. Oceanogr.* 111, 1–9. doi: 10.1016/j.dsr2.2014.11.001
- Brandt, A., Malyutina, M. V., Alalykina, I. L., Brenke, N., Chernyshev, A. V., Elsner, N. O., et al. (2013). The German-Russian deep-sea expedition KuramBio (Kurile-Kamchatka Biodiversity Study) to the Kurile-Kamchatka Trench and abyssalplain on board of the R/V *Sonne*, 223rd Expedition (July 21th – September 7th 2012). *Cruise. Rep. POS. 456. Kiel. – 2. Reykjavik.* 20.07. – 04.08.2013. 456, 1–100. doi: 10.13140/RG.2.2.17251.76322
- Brandt, A., Martínez Arbizu, P., Malyutina, M. V., Alalykina, I. L., Bober, J., et al. (2016). *RV Sonne SO-250 Cruise Report (Kuril Kamchatka Biodiversity Studies).*
- Carr, L. A., Boyer, K. E., and Brooks, A. J. (2011). Spatial patterns of epifaunal communities in San Francisco bay eelgrass (*Zostera marina*) beds. *Mar. Ecol.* 32, 88–103. doi: 10.1111/j.1439-0485.2010.00411.x
- Castresana, J. (2000). Selection of conserved blocks from multiple alignments for their use in phylogenetic analysis. *Mol. Biol. Evol.* 17, 540–552. doi: 10.1093/oxfordjournals.molbev.a026334
- Clark, M. S. (2020). Molecular mechanisms of biomineralization in marine invertebrates. *J. Exp. Biol.* 223, 88–103. doi: 10.1242/jeb.206961
- Coleman, C. O. (2003). "Digital inking": How to make perfect line drawings on computers. *Org. Divers. Evol.* 3, 303–304. doi: 10.1078/1439-6092-00081
- Dojiri, M., and Sieg, J. (1997). Taxonomic atlas of the soft-bottom benthic fauna of the Santa Maria Basin and Western Santa Barbara Channel. pp. 181–268
- Di Franco, D., Linse, K., Griffiths, H. J., and Brandt, A. (2021). Drivers of abundance and spatial distribution in Southern Ocean peracarid Crustacea. *Ecol. Indic.* 128, 1–9. doi: 10.1016/j.ecolind.2021.107832
- Ewers-Saucedo, C. (2019). Evaluating reasons for biased sex ratios in Crustacea. *Invertebr. Reprod. Dev.* 63, 222–230. doi: 10.1080/07924259.2019.1588792
- Frutos, I., Kaiser, S., Pułaski, Ł., Studzian, M., and Błażewicz, M. (2022). Challenges and advances in the taxonomy of deep-sea Peracarida: From traditional to modern methods. *Front. Mar. Sci.* 9 799191. doi: 10.3389/fmars.2022.799191
- Gamo, S. (1984). A new remarkably giant tanaid *Gigantapseudes maximus* sp. nov. (Crustacea) from the abyssal depths far off southeast of Mindanao, the Philippines. *Sci. Rep. Yokohama. Natl. Univ. Sect. II. Biol. Geol.* 31, 1–12.
- Garm, A. (2004). Revising the definition of the crustacean seta and setal classification systems based on examinations of the mouthpart setae of seven

- species of decapods. *Zool. J. Linn. Soc* 142, 233–252. doi: 10.1111/j.1096-3642.2004.00132.x
- Gellert, M., Bird, G. J., Stepien, A., and Studzian, M. (2022). A hidden diversity in the Atlantic and the SE Pacific: Hamatipedeidae n. fam. (Crustacea: Tanaidacea). *Front. Mar. Sci.* 8. doi: 10.3389/fmars.2021.773437
- Gellert, M., Palero, F., and Błażewicz, M. (in press) Mislabeling and nomenclatorial confusion of *Typhlotanais sandersi* Kudinova-Pasternak, 1985 (Crustacea: Tanaidacea) and establishment of a new genus. *PeerJ*.
- Golovan, O. A., Błażewicz-Paszkwyc, M., Brandt, A., Budnikova, L. L., Elsner, N. O., Ivin, V. V., et al. (2013). Diversity and distribution of peracarid crustaceans (Malacostraca) from the continental slope and the deep-sea basin of the Sea of Japan. *Deep. Res. Part II. Top. Stud. Oceanogr.*, 86, 66–78. doi: 10.1016/j.dsr2.2012.08.002
- Grebmeier, J. M., Cooper, L. W., Feder, H. M., and Sirenko, B. I. (2006). Ecosystem dynamics of the Pacific-influenced Northern Bering and Chukchi Seas in the Amerasian Arctic. *Prog. Oceanogr.* 71, 331–361. doi: 10.1016/j.pocean.2006.10.001
- Hansen, H. J. (1913). Crustacea Malacostraca. II. IV. The order Tanaidacea. *Danish. Ingolf-Expedition*. 3, 1–145.
- Hassack, E., and Holdich, D. M. (1987). The tubicolous habit amongst the Tanaidacea (Crustacea, Peracarida) with particular reference to deep-sea species. *Zool. Scr.* 16, 223–233. doi: 10.1111/j.1463-6409.1987.tb00069.x
- Highsmith, R. C. (1985). Floating and algal rafting as potential dispersal mechanisms in brooding invertebrates. *Mar. Ecol. Prog. Ser.* 180, 235–251. doi: 10.3354/meps025169
- Hilário, A., Metaxas, A., Gaudron, S. M., Howell, K. L., Mercier, A., Mestre, N., et al. (2015). Estimating dispersal distance in the deep sea: Challenges and applications to marine reserves. *Front. Mar. Sci.* 2. doi: 10.3389/fmars.2015.00006
- Jążdżewska, A. M., Brandt, A., Martínez Arbizu, P., and Vink, A. (2021a). Exploring the diversity of the deep sea—four new species of the amphipod genus *Oedicerina* described using morphological and molecular methods. *Zool. J. Linn. Soc* 194, 1–45. doi: 10.1093/zoolinnean/zlab032
- Jążdżewska, A. M., Horton, T., Hendrycks, E., Mamos, T., Driskell, A. C., Brix, S., et al. (2021b). Pandora's box in the deep sea – intraspecific diversity patterns and distribution of two congeneric scavenging amphipods. *Front. Mar. Sci.* 8. doi: 10.3389/fmars.2021.750180
- Jążdżewska, A. M., and Mamos, T. (2019). High species richness of Northwest Pacific deep-sea amphipods revealed through DNA barcoding. *Prog. Oceanogr.* 178, 1–15. doi: 10.1016/j.pocean.2019.102184
- Jakiel, A., Palero, F., and Błażewicz, M. (2019). Deep Ocean seascape and Pseudotanaididae (Crustacea: Tanaidacea) diversity at the Clarion-Clipperton Fracture Zone. *Sci. Rep.* 9, 1–49. doi: 10.1038/s41598-019-51434-z
- Jakiel, A., Palero, F., and Błażewicz, M. (2020). Secrets from the deep: Pseudotanaididae (Crustacea: Tanaidacea) diversity from the Kuril–Kamchatka Trench. *Prog. Oceanogr.* 183, 1–20. doi: 10.1016/j.pocean.2020.102288
- Jakiel, A., Stepien, A., and Błażewicz, M. (2018). A tip of the iceberg—Pseudotanaididae (Tanaidacea) diversity in the North Atlantic. *Mar. Biodivers.* 48, 859–895. doi: 10.1007/s12526-018-0881-x
- Johnson, S. B., and Attramadal, Y. G. (1982). A functional-morphological model of *Tanais cavolinii* Milne-Edwards (Crustacea, Tanaidacea) adapted to a tubicolous life-strategy. *Sarsia* 67, 29–42. doi: 10.1080/00364827.1982.10421329
- Kaiser, S., Brix, S., Kihara, T. C., Janssen, A., and Jennings, R. M. (2018). Integrative species delimitation in the deep-sea genus *Thaumastosoma* Hessler, 1970 (Isopoda, Asellota, Nannoniscidae) reveals a new genus and species from the Atlantic and central Pacific abyss. *Deep. Res. Part II. Top. Stud. Oceanogr.* 148, 151–179. doi: 10.1016/j.dsr2.2017.05.006
- Kato, K., and Standley, D. M. (2013). MAFFT multiple sequence alignment software version 7: Improvements in performance and usability. *Mol. Biol. Evol.* 30, 772–780. doi: 10.1093/molbev/mst010
- Kolesnik, A. N., Kolesnik, O. N., Sattarova, V. V., Karabtsov, A. A., and Yaroshchuk, E. I. (2019). Color and chemical composition of bottom sediments from the Kuril Basin (Sea of Okhotsk) and the Kuril–Kamchatka Trench area (Northwest Pacific). *Prog. Oceanogr.* 178, 1–13. doi: 10.1016/j.pocean.2019.102197
- Kudinova-Pasternak, R. K. (1966). Tanaidacea (Crustacea) of the Pacific ultra-abysals. *Crustaceana* 45, 518–534.
- Kudinova-Pasternak, R. K. (1970). Tanaidacea of the Kurile-Kamchatka Trench. *Akad. Nauk. SSSR*. 86, 341–380.
- Kudinova-Pasternak, R. K. (1973). Tanaidacea (Crustacea, Malacostraca) collected on the R/V *Vitjas* in regions of the Aleutian Trench and Alaska. *Trudy Instituta Okeanologii, Akademiya Nauk* 9, 141–168.
- Kudinova-Pasternak, R. K. (1876). Additional notes on the fauna of Tanaidacea (Crustacea, Malacostraca) of the deepwater trench. *Trudy Instituta Okeanologii Akademiya Nauk SSSR* 99, 11–125.
- Kudinova-Pasternak, R. K., and Pasternak, F. A. (1978). Deep-sea Tanaidacea, Caribbean Sea, Puerto Rico Trench. *Trudy Instituta Okeanologii, Akademiya Nauk SSSR* 113, 178–197.
- Kudinova-Pasternak, R. K. (1984). Tanaidacea (Crustacea, Malacostraca) Japanskogo Morja. *Zool. Zhurnal*. 53, 828–837.
- Kudinova-Pasternak, R. K. (1985). Tanaidacea (Crustacea, Malacostraca) collected on the summit and at foot of Great-Meteor Seamount. *Zool. Zhurnal*. 120, 52–64.
- Kumar, S., Stecher, G., Li, M., Knyaz, C., and Tamura, K. (2018). MEGA X: Molecular evolutionary genetics analysis across computing platforms. *Mol. Biol. Evol.* 35, 1547–1549. doi: 10.1093/molbev/msy096
- Larsen, K., Błażewicz-Paszkwyc, M., and Cunha, M. R. (2006). Tanaidacean (Crustacea: Peracarida) fauna from chemically reduced habitats - The Lucky Strike hydrothermal vent system, Mid-Atlantic Ridge. *Zootaxa* 36 (1187), 1–36.
- Larsen, K. (2005). *Deep-sea Tanaidacea (Peracarida) from the Gulf of Mexico. Crustaceana monographs* (Leiden: Brill), 1–390.
- Larsen, K., and Shimomura, M. (2007). Tanaidacea (Crustacea: Peracarida) from Japan III. The deep trenches: the Kurile-Kamchatka Trench and Japan Trench. Eds. K. Larsen and M. Shimomura. Tanaidacea (Crustacea: Peracarida) From Japan III. The Deep Trenches: The Kurile-Kamchatka Trench and Japan Trench. *Zootaxa* 1599, 5–12.
- Leprieur, F., Descombes, P., Gaboriau, T., Cowman, P. F., Parravicini, V., Kulbicki, M., et al. (2016). Plate tectonics drive tropical reef biodiversity dynamics. *Nat. Commun.* 7, 1–8. doi: 10.1038/ncomms11461
- Lilljeborg, W. (1864). Bidrag til kändedomen om de inom Sverige och Norrige förekommande Crustaceer af Isopodernas underordning och Tanaidernas familj. *Inbjudningsskrift till Åhörande af de Offentliga Föreläsninge* 1865, 1–31.
- Malyutina, M. V., Brandt, A., and Ivin, V. V. (2015). *The Russian-German deepsea expedition SokhoBio (Sea of Okhotsk Biodiversity Studies) to the Burile Basin of the Sea of Okhotsk on board of the R/V Akademik M.A. Lavrentyev 71st Cruise, July 6th - August 6th (The Cruise Report)*, 1–52.
- McCallum, A. W., Woolley, S. N. C. C., Błażewicz-Paszkwyc, M., Brown, J., Gerken, S., Kloser, R., et al. (2015). Productivity enhances benthic species richness along an oligotrophic Indian Ocean continental margin. *Glob. Ecol. Biogeogr.* 24, 462–471. doi: 10.1111/geb.12255
- McLelland, J. A. (2007). “Family Pseudotanaidae Sieg, 1976,” Eds. K. Larsen and M. Shimomura Tanaidacea (Crustacea: Peracarida) From Japan III. The Deep Trenches: The Kurile-Kamchatka Trench and Japan Trench. *Zootaxa* 1599, 87–99. doi: 10.11664/zootaxa.1599.1.5
- Messing, C. G. (1976). *Neotanais persephone*, a new species of hadal tanaidacean (Crustacea: Peracarida). *Bull. Mar. Sci.* 27, 511–519.
- Morse, J. W., and Mackenzie, F. T. (1990). *Geochemistry of sedimentary carbonates* (Amsterdam: Elsevier), 1–707.
- Palero, F., Guerao, G., and Abelló, P. (2008). Morphology of the final stage phyllisoma larva of *Scyllarus pygmaeus* (Crustacea: Decapoda: Scyllaridae), identified by DNA analysis. *J. Plankton. Res.* 30, 483–488. doi: 10.1093/plankt/fbn012
- Pálke, H., Lyle, M. W., Nishi, H., Raffi, I., Ridgwell, A., Gamage, K., et al. (2012). A Cenozoic record of the equatorial Pacific carbonate compensation depth. *Nature* 488, 609–614. doi: 10.1038/nature11360
- Pitz, K. M., and Sierwald, P. (2010). Phylogeny of the millipede order Spirobolida (Arthropoda: Diplopoda: Helminthomorpha). *Cladistics* 26, 497–525. doi: 10.1111/j.1096-0031.2009.00303.x
- Poore, G. C. B., Avery, L., Błażewicz-Paszkwyc, M., Brown, J., Bruce, N. L., Gerken, S., et al. (2015). Invertebrate diversity of the unexplored marine western margin of Australia: Taxonomy and implications for global biodiversity. *Mar. Biodivers.* 45, 271–286. doi: 10.1007/s12526-014-0255-y
- Renema, W., Bellwood, D. R., Braga, J. C., Bromfield, K., Hall, R., Johnson, K. G., et al. (2008). Hopping hotspots: Global shifts in marine biodiversity. *Science* 321, 654–657. doi: 10.1126/science.1155674
- Rewicz, A., Bomanowska, A., Magda, J., and Rewicz, T. (2017). Morphological variability of *Consolida regalis* seeds of south-eastern and central Europe. *Syst. Biodivers.* 15, 25–34. doi: 10.1080/14772000.2016.1216017
- Riehl, T., Brenke, N., Brix, S., Driskell, A. C., Kaiser, S., and Brandt, A. (2014). Field and laboratory methods for DNA studies on deep-sea isopod crustaceans. *Polish. Polar. Res.* 35, 203–224. doi: 10.2478/popore-2014-0018
- Sars, G. O. (1882). Revision af gruppen: Isopoda Chelifera med karakteristisk af nye herhen hørende arter og slægter. *Archiv for Mathematik Og Naturvidenskab* 7, 1–54. <http://biostor.org/reference/129114>
- Saeedi, H., and Brandt, A. (2020). Foreword, in *Biogeographic atlas of the deep NW Pacific Fauna*. Eds. H. Saeedi and A. Brandt (Sofia: Pensoft Publishers), 9–22. doi: 10.3897/ab.e51315

- Saeedi, H., Costello, M. J., Warren, D., and Brandt, A. (2019). Latitudinal and bathymetrical species richness patterns in the NW Pacific and adjacent Arctic Ocean. *Sci. Rep.* 9, 1–10. doi: 10.1038/s41598-019-45813-9
- Sattarova, V. V., and Artemova, A. V. (2015). Geochemical and micropaleontological character of deep-sea sediments from the Northwestern Pacific near the Kuril–Kamchatka Trench. *Deep. Res. Part II. Top. Stud. Oceanogr.* 111, 10–18. doi: 10.1016/j.dsr2.2014.10.030
- Segadilha, J. L., Gellert, M., and Błażewicz, M. (2018). A new genus of Tanaidacea (Peracarida, Typhlotanaidae) from the Atlantic slope. *Mar. Biodivers.* 48, 915–925. doi: 10.1007/s12526-018-0856-y
- Segadilha, J. L., Serejo, C. S., and Błażewicz, M. (2019). New species of Typhlotanaidae (Crustacea, Tanaidacea) from the Brazilian coast: genera *Hamatipeda*, *Meromonakantha* and *Paratyphlotanais*, with description of *Targarynella* gen. nov. *Zootaxa*. 4661, 309–342. doi: 10.11646/zootaxa.4661.2.4
- Segadilha, J. L., and Serejo, C. S. (2022). New insights gained from museum collections: new deep-sea species of *Typhlotanais* (Tanaidacea, Typhlotanaidae) from Brazil. *European Journal of Taxonomy* 820(1), 1–54. doi: 10.5852/ejt.2022.820.1791
- Sieg, J. (1983). Tanaidomorpha (Crustacea: Tanaidacea) from the Ross Sea, Antarctica. *Journal of the Royal Society of New Zealand* 13 (4), 395–418.
- Sieg, J. (1984). Neuere Erkenntnisse zum natürlichen System der Tanaidacea. *Zoologica* 136, 100–132.
- Sieg, J. (1986). Tanaidacea (Crustacea) von der Antarktic und Subantarktis. II. Tanaidacea gesammelt von Dr. J. W. Wägele während der Deutschen Antarktis Expedition 1983. *Mitteilungen aus dem Zool. Museum Univ. Kiel* II, 1–80.
- Sirenko, B. I. (2013). Check-list of species of free-living invertebrates of the Russian Far Eastern Seas. Class Ophiuroidea. *Russ. Acad. Sci. Zool. Institute. St. Petersburg. Russ.* 75–83, 1–258.
- Stepień, A., Józwiak, P., Jakiel, A., Pelczyńska, A., and Błażewicz, M. (2022). Diversity of Pacific *Agathotanis* (Peracarida: Tanaidacea). *Front. Mar. Sci.* 8, 741536. doi: 10.3389/fmars.2021.741536.
- Stepień, A., Pabis, K., and Błażewicz, M. (2019). Tanaidacean faunas of the Sea of Okhotsk and northern slope of the Kuril–Kamchatka Trench. *Prog. Oceanogr.* 178, 1–11. doi: 10.1016/j.pocean.2019.102196
- Talavera, G., and Castresana, J. (2007). Improvement of phylogenies after removing divergent and ambiguously aligned blocks from protein sequence alignments. *Syst. Biol.* 56, 564–577. doi: 10.1080/10635150701472164
- Tattersall, (1904). Some new and rare Isopoda taken in the British area. *Report of the Seventy-Fourth Meeting of the British Association for the Advancement of Science* 1904, 601–602.
- Thomas, W. J. (1970). The setae of *Austropotamobius pallipes* (Crustacea: Astacidae). *J. Zool.* 161, 91–142. doi: 10.1111/j.1469-7998.1970.tb02899.x
- Wolff, T. (1956). Crustacea Tanaidacea from depths exceeding 6000 metres. *Deep. Sea. Res. Oceanogr.* 17, 983–1003. doi: 10.1016/0011-7471(70)90049-5
- Wolfram Research Inc (2020). *Mathematica Edition: Version 12.1*.